Article

Circadian Clock Contributes to Modulate Salinity Stress-Responsive Antioxidative Mechanisms and Chloroplast Proteome in *Spinacia oleracea*

Ajila Venkat [1,2], Dong-Won Bae [3] and Sowbiya Muneer [1,*]

1   Horticulture and Molecular Physiology Lab, School of Agricultural Innovations and Advanced, Learning, Vellore Institute of Technology, Vellore 632014, India
2   School of Biosciences and Technology, Vellore Institute of Technology, Vellore 632014, India
3   Central Instrument Facility, Gyeongsang National University, Jinju 52828, Republic of Korea
*   Correspondence: sowbiya.muneer@vit.ac.in or sobiyakhan126@gmail.com

Abstract: Extreme abiotic stresses such as drought, salinity, and temperature reduce crop productivity significantly and pose a serious threat to the area of land used for agriculture. Therefore, there is a pressing need to create crops that can thrive in these circumstances. It has been noted that plants can maintain defense mechanisms during any environmental changes and anticipate diurnal patterns correct to a circadian-based clock. Therefore, the main aim of this study was to investigate the role of circadian core oscillators in response to salinity stress in an important vegetable crop, spinach, and obtain evidence to better understand salinity stress adaptation for crop productivity. Therefore, the current study was carried out to examine the circadian clock-based (morning–evening loop) salinity stress defense mechanism in spinach (*Spinacia oleracea*), a leafy vegetable crop with significant economic importance and health benefits. In the presence of dawn and dusk, the circadian clock-based defense mechanism was observed using the genotypes "Delhi Green" and "Malav Jyoti." A photoperiodic rhythm consists of 4-h intervals for 12 h (morning–evening loop) in spinach was demonstrated under the salinity stress treatments (20 mM and 50 mM). The clock-controlled a large fraction of growth parameters such as plant height, biomass, and root-shoot ratio under salinity stress. Conversely, salinity stress resulted in upregulation of antioxidative parameters such as superoxide dismutase, ascorbate peroxidase, catalase, and other stress markers such as thiobarbituric acid reactive substances, proline content, and localizations of H_2O_2 and O_2^{-1} but was altered and maintained at a certain photoperiodic time interval of the circadian clock. In distinction to results observed from antioxidative measurements performed with an early and late circadian duration of salt-treated plants, 10 am and 2 pm were revealed to be the rhythmic times for controlling salinity stress. Likewise, comprehensive measurements of the photosynthetic system under salinity stress at specific photoperiodic circadian time intervals, including net-photosynthetic rate, transpiration, stomatal conductance, PSII quantum yield, and stomata structure, were made at 10 am and 2 pm. The salinity stress response was down-streamed and the clock also regulated chloroplastic protein expression. Thus, according to our findings, photoperiodic circadian rhythms, particularly the morning–evening loop, enhanced plant survival rates by modulating cellular antioxidant mechanisms and chloroplastic proteins that further helped to reduce the effects of salinity stress.

Keywords: ROS scavenging mechanism; circadian oscillator; thylakoid proteome; salt stress; photoperiodism; rhythmic hours

1. Introduction

Amongst all abiotic stress conditions, salt stress is one of the most critical abiotic stresses when it comes to plant growth [1]. The major effects of salinity are poor drainage and waterlogging, which further lead to a lack of plant productivity and lower overall productivity of agricultural land [2]. The effects of salt on the soil reduce the area used for

irrigated land. This has been expressed in the form of percentage with various countries facing the same issue. In India, during 2001, the reduction was about 27%, 13% in Israel, 15% in China, 20% in Australia, 28% in Pakistan, 30% in Egypt, and 50% in Iraq [3]. This indicates that the agricultural areas in India are facing a moderate increase in soil salinity that affects crop production and development. This evolving issue of salt stress on soils and crops has the potential to cause adverse effects in the near future due to certain naturally occurring variations such as the unstable climatic conditions and salt water irrigation, as well as the effects of global warming, pollution and uncontrolled or unrestricted usage of chemical or biological fertilizers and pesticides [4,5].

Excess salt concentration in plants leads to an increase in osmotic stress and formation of an ionic imbalance along with the deposition of toxic ions such as chloride (Cl^-) ions [6] and, most seriously, sodium (Na^+) ions [7]. Increases in the level of salinity lead to osmotic stress, an asymmetry in ions and further detrimental effects on biochemical processes, biomass, and morphological characteristics of the plants and can also lead to plant death. During unfavorable salinity stress conditions, plants assemble soluble sugars and proline, which are known to be an osmolytes (or osmo-regulators), to preserve the plant cells [8]. The increase in the salt quantity causes a conflict with transportation and uptake of nutrients; salt stress has a negative effect on the process of photosynthesis. The presence of salt content in the soil influences osmotic stress, which is a crucial factor in oxidative stress due to the disproportionate stimulation of reactive oxygen species (ROS) and the suppression role of anti-oxidants [9]. The other main processes such as lipid metabolism and protein synthesis are also affected. Hydrogen peroxide (H_2O_2), superoxide radicals (O_2^-) and singlet oxygen are harmful molecules which are known to be forms of ROS [10,11].

ROS can also cause cellular damage to almost all macro molecules present in a crop, even including DNA. The harmful effects of ROS are prevented by either enzymatic [12] or non-enzymatic [13] anti-oxidative processes such as superoxide dismutase (SOD), catalase (CAT), ascorbate peroxidase (APX), glutathione reductase (GR), ascorbic acid (AsA) and phenolic compounds [14–16]. The increase in the ratio of Na^+ or K^+ reduces certain metabolic processes including PSII quantum yield, transpiration and stomatal conductance [17]. The reduction in the function of the Calvin cycle indirectly decreases the rate of net photosynthesis through a reduction in carbon dioxide intake and the limitation of photosynthetic pigments which include chlorophyll [18]. The increase in concentration of ROS inside the cells reduces the anti-oxidant properties which end up in the process of lipid peroxidation (LPO). Eventually, the degeneration of protein, nucleic acids and lipids takes place due to the formation of free radicals. The LPO (or malonaldehyde content (MDA)) has a major effect on cell permeability and cell membrane structure [18,19].

Circadian clocks are biological oscillators that run 24 h a day and enable organisms to anticipate predictable daily changes brought on by the rotation of the earth. Clocks have been found among other creatures such as cyanobacteria, fungi, insects, and mammals [20]. There is no requirement for a clock for plant viability, and arrhythmic mutants can still arise [21]. Despite this, there is strong support for the idea that plants benefit greatly from having a clock that is well-tuned to the cycles of day and night. For instance, in competition studies, plants with clocks that matched their rhythmic environment outperformed others [22]. This might be explained, at least in part, by how the clock controls how well starch is used at night to prevent famine before dawn [23–26]. Recent evidence suggests, however, that the circadian clock may contribute to plant fitness by improving its ability to withstand abiotic stress [27–32]. Therefore, the current study was designed to examine evidence that the plant circadian clock could be such a system.

Spinach (*Spinacia oleracea*) is a flexibly used, leafy, dark green colored, edible vegetable crop containing a good source of vitamins, such as vitamin-C, pro vitamin-A (beta-carotene) and folate [33]. It is rich in protein, minerals, iron, calcium, phosphorous, potassium, sodium and carotenoids, especially lutein. It also has anti-inflammatory properties and anti-oxidant properties along with active compounds which include flavonoids. As a result, the vegetable has high nutritional value. Freshly harvested leaves of spinach have roughly one gram

of total flavonoid present per kilogram. The presence of flavonoids in spinach was first described by Weatherby and Cheng in 1943 [34]. The cultivation of spinach takes place all over the world, in almost 60 countries. The major spinach producing countries apart from India are the United States, Indonesia, Japan, Iran, China, and Turkey [35]. Generally, spinach is a directly seeded crop. It is known to be native to central Asia and has been cultivated for more than 1500 years [36]. According to a previous study [37], moderate salt stress in spinach crops suppresses photosynthesis by limiting the diffusion of carbon dioxide due to decreases in mesophyll and stomatal conductance; however, this does not affect the physiochemical and biochemical properties of spinach leaves. A drastic increase in salt level can diminish the carbon metabolism and electron transport chain in photosynthesis. The effect of salt stress can be reversed and the photosynthesis activity restored through irrigating the spinach crop in normal water (without the presence of salt) [38].

The current research is a comparative analysis on the effects of salinity stress in different concentrations (20 mM and 50 mM) on spinach crop (*Spinacia oleracea*) genotypes (Malav Jyoti and Delhi Green) based upon a 12 h circadian clock at time intervals of about 4 h, for instance, 6 am, 10 am, 2 pm and 6 pm on day 5 and day 10 (early and late stress days). The present study helps in the analysis of salt resistant and salt sensitive spinach genotypes with significant measurements of physiological parameters (which include the photosynthetic parameters), oxidative parameters and cytotoxic analysis, thylakoid and chloroplast proteomes. To date there are no reports on the comparative study of these spinach genotypes with these two saline concentrations. This study could further help in the investigation of plant sustainability under salt stress conditions in a field-level analysis using specific agricultural techniques. From our study we hypothesize that circadian core oscillators particularly play a critical role in mitigating salinity stress by modulating physiological parameters such as photosynthesis, antioxidative mechanisms, and the chloroplast proteome specifically at certain times in the circadian cycle (10 am and 2 pm). From this study, we also hypothesize the possible importance in further investigating the basis and significance of circadian-gated salinity stress responses under fluctuating circadian rhythmic conditions and the probable significance of exploiting an effective way to improve spinach production under salinity stress.

2. Material and Methods

2.1. Plant Materials, Growth Conditions, Treatments and Sample Storage

The genotypes of spinach (*Spinacia oleracea*) 'Malav Jyoti' and 'Delhi Green' were obtained from an Indian Government seed shop (Rajamanickam Agro Service-Seed Retailers). These seeds were sown in grow bags after carrying out a process of surface sterilization using a mixture containing 5% sodium hypochlorite for about 30 min and then further washing using distilled water. The soil used for sowing the seeds consisted of red soil, sand and vermi-compost in a ratio of 1:1:1. The plants were grown and maintained under polyhouse conditions in the School of Agricultural Innovations and Advanced Learning, Vellore Institute of Technology, Vellore, India. The grow bags (Bio Blooms, Coimbatore, India) had the following dimensions: 24 cm in height, 24 cm in width, and 40 cm in length). These grow bags had the capacity to accommodate 4.5 kilograms of soil mixture, but here they filled with about 3.5 kilograms of the above-mentioned soil composition, which was about three-quarters of the grow bags' capacity. In total, 30 grow bags were filled for a set of germinations, with 15 grow bags allocated to the genotype Malav Jyoti (MJ) and the rest of the 15 grow bags allocated to the other genotype, Delhi Green (DG).

To treat the plants with salinity or salt stress, sodium chloride (NaCl) was used in two different concentrations: 20 mM and 50 mM. The above-mentioned 15 grow bags were separated into 3 groups: 5 bags for the control, 5 bags for 20 mM of NaCl, and 5 bags for the 50 mM of NaCl treatment (in each experiment, there were three biological replicates with one bag representing one replicate and the remaining two bags kept for either taking photographs or obtaining extra samples). Each grow bag had approximately 6 to 8 sown seeds, which went through a further thinning process once germination occurred;

in addition, each seed was sown at a depth of about 1 cm from the upper surface of the soil in the bag. The salt treatments, consisting of a volume of about 100 mL per grow bag, were applied between 30 and 35 days, once after the seeds were sown and once before the plants reached their vegetative or mature stage. The day when the seeds were sown was considered as day 0. Similarly, the day when the plants were treated with salt stress (by soil irrigation technique) was considered as day 0, so the next consecutive day was designated as day 1 for both plant germination and treatments. The plants were observed and the photographs were taken on alternate days. Leaf samples were collected at intervals of about 4 h (on the basis of the morning–evening circadian loop), which were exactly at the times of 6 am, 10 am, 2 pm and 6 pm of both day 5 and day 10. Immediately after collection, the samples were stored at $-80\ °C$ in a deep freezer. Analytical and molecular level grade chemicals were used to perform the further experiment, and three samples were tested for each plant.

2.2. Growth Analysis

On day 5 and day 10 of the salt treatment, the plants were removed carefully from the grow bags. These plants were then used for measuring plant and root length on the same day. Photographs of the control, 20 mM NaCl and 50 mM NaCl plants were captured to show plant height with a scale provided alongside.

2.3. Biomass and Relative Water Content (RWC)

The whole plant samples were collected from grow bags, and the root was washed gently with distilled water. The fresh biomass was noted by weighing the samples using a digital weighing balance. The same samples were kept in hot air oven for exactly 2 days under 65–70 °C constant temperature, after which, the dry biomass was measured as mentioned in Al Murad and Muneer [18] and was calculated using the formula **Biomass = FB – DB**, where FB is fresh biomass and DB is dry biomass.

Leaf samples were used to measure the percentage relative water content, according to the methods of Turner et al. [39]. The fresh leaves were collected and washed, after which, the fresh biomass (FB) was measured. These leaves were then soaked in distilled water for 2 to 4 h and further weighed to measure the turgid biomass (TB). The same leaf samples were kept in hot air oven for 2 days under a constant temperature of 65–70 °C to measure the dry biomass (DB) of each leaf. It was then calculated based on the formula relative water content (RWC) **% = (FB — DB)/(TB — DB) ∗ 100.**

2.4. Photosynthetic Measurements

The soil plant analysis development (SPAD) meter (Konika Minolta, Tokyo, Japan), which is a portable instrument, was used to measure the net photosynthesis rate, transpiration rate and the stomatal conductance in the treatment and control plants [40].

The photosystem II (PS-II) quantum yield was measured using an instrument known as a pulse amplitude modulator (PAM) 2000 m (Heinz Walz GmbH, Xarges 40860, Weiheim, Germany) which measures the chlorophyll fluorescence (Fv/Fm). A 1 cm*1 cm leaf sample was kept in dark conditions for about 20 to 30 min. After this incubation period, readings were performed to determine the initial fluorescence yield (F0) and maximum fluorescence yield (Fm). The chlorophyll fluorescence was then calculated as (Fv/Fm) = (Fm − F0)/Fm [41].

2.5. Photosynthetic Pigment Analysis

To identify the quantities of photosynthetic pigments (chlorophyll a, chlorophyll b, carotenoid, and total chlorophyll) present in the sample, a 1-g leaf sample was taken (using a weighing balance from HIMEDIA, Aczet Pvt. Ltd., Mumbai) and placed in a separate glass test tube. Then, 5 mL of DMSO (Dimethyl Sulfoxide), which removes the pigments from the leaf samples [42], was added to each test tube. The samples were then incubated for 60 min in a water bath under 65 °C. The absorbance of these leached pigments was

measured at the wavelengths of 480 nm, 510 nm, 645 nm and 663 nm, using a UV-Visible spectrophotometer. Thus, the pigment abundances were calculated with the respective formulae as mentioned in [43] with the unit of mg/g fresh weight.

2.6. Proline and MDA Content

The estimation of proline content was performed according to the methods of a previous study [44]. Leaf samples of 300 mg of were taken and homogenized with 5 mL of 3% sulfosalicylic acid. The tubes containing the homogenized samples were centrifuged (using NEYA 16R REMI) at 3300 rpm for 20 min at 4 °C. Almost 2 mL of supernatant was placed in separate test tubes. Along with the aliquot, 2 mL of acid ninhydrin solution (containing glacial acetic acid and ortho-phosphoric acid) and 2 mL of glacial acetic acid were added. The test tubes were incubated in a boiling water bath (Technico Seriological Water Bath, Chennai) at 100 °C for 60 min. To terminate the reaction the test tubes were placed in ice, immediately after incubation. Then, 4 mL of toluene was added to each test tube containing the mixture. The test tubes were further gently mixed through vortex and kept at room temperature. The absorbance was observed under a wavelength of 520 nm using toluene as a blank.

The analysis of malondialdehyde (MDA) content was performed using the thiobarbituric acid reactive substance (TBARS) assay [45]. Approximately, 0.4 g of fresh leaf sample was taken and the exact weight of sample measured was recorded for further calculation. The measured sample was ground with 5 mL of 1% trichloroacetic acid (TCA) in a pre-cooled mortar and pestle. The homogenate was centrifuged at 7000 rpm for 5 min. Along with the 1 mL of supernatant, 4 mL of 0.5% TBA (in 20% TCA) was added to a separate test tube. The sample mixture was further incubated in a boiling water bath at 95 °C for 30 min. It was then quickly placed in ice to stop the reaction. The supernatant was used to read the OD at 532 nm and corrected for unspecific turbidity by subtracting the results received from the OD at 600 nm using a UV-Vis spectrophotometer.

2.7. Histochemical Staining of H_2O_2 and O_2^-

The analysis of hydrogen peroxide (H_2O_2) and superoxide radicles (O_2^-) localization was performed using the method of a previous study [46] with minor modifications.

For the analysis of in situ localization of H_2O_2, freshly collected leaf samples were immersed in 1% 3, 3′-diaminobenzidine (DAB) solution prepared in Tris-HCl buffer with pH 6.5. The samples were further vacuum infiltrated for about 5 min and then incubated at room temperature for 12 h in dark conditions. The leaves were immersed and bleached with 95% ethanol in a boiling water bath for 1 h to visualize the brown spots. Subsequently, photographs were taken using a digital camera.

For the localization of O_2^-, the fresh leaves were immersed in 0.1% Nitroblue tetrazolium (NBT) solution prepared in 20 mM phosphate buffer (pH 6.5) containing 20 mM of Sodium azide. The samples were vacuum infiltrated for 5 min and incubated at room temperature for 15 h in dark conditions. The leaves were then immersed and bleached in boiling 95% ethanol for 1 h 15 min. The appearance of blue formazan precipitate was visualized and photographed.

2.8. Anti-Oxidant Enzymatic Assays and Their Isozyme Analysis

For estimating the superoxide dismutase (SOD) enzyme activity [47], a 200 mg fresh leaf sample was taken and homogenized with 2 mL of extraction buffer containing 0.5 M phosphate buffer (K_2HPO_4 (dibasic potassium phosphate), KH_2PO_4 (potassium dihydrogen phosphate) (pH 7.5), 1% of PVP (polyvinylpyrrolidone), 1% of Triton-X 100, and 1 mM EDTA (ethylenediamine tetraacetic acid) using a pre-cooled mortar and pestle. The homogenates were centrifuged at 15,000 rpm at 4 °C and the supernatant was collected for further analysis. Along with the supernatant, 1.5 mL of reaction buffer containing 0.1 M phosphate buffer (pH 7.8), 0.1 M sodium carbonate, 200 mM methionine solution, 2.25 mM NBT solution, 3 mM EDTA, 60 μM riboflavin and distilled water. One set of this mixture was

incubated in dark conditions at room temperature and other set was incubated under a 15 W fluorescent lamp light for 10 min. A blank was maintained in both conditions with all components except the enzyme extract. The absorbance of the sample was determined at 560 nm. The percentage reduction in color corresponds to a unit of enzyme activity, which was expressed as unit of enzyme mg^{-1} protein h^{-1}.

To determine catalase (CAT) enzyme activity [48], 200 mg of leaf sample was homogenized with 2 mL of 0.5 M extraction buffer (pH 7.5) consisting of phosphate buffer (K$_2$HPO$_4$, KH$_2$PO$_4$), 1% PVP, 1% Triton-X100 and 1 mM of EDTA. The gound samples were centrifuged at 10,000 rpm for 20 min at 4 °C. Then, the supernatant was added to a separate tube add reaction buffer containing phosphate buffer (pH 7.3) was added. Finally, 3 mM of H$_2$O$_2$ (enzyme substrate) was added and mixed manually, making the total volume of the mixture 1 mL. The absorbance was measured at 240 nm for 3 min at 30 s time intervals (E = 39.4 mM^{-1} cm^{-1}).

For determining ascorbate peroxidase (APX) enzyme activity [49], 200 mg leaf material was collected and homogenized with 2 mL of 0.5 M extraction buffer (pH 7.5), which is composed of KH$_2$PO$_4$ and K$_2$HPO$_4$ phosphate buffer, 1% PVP, 1% Triton-X 100 and 1 mM of EDTA. The mixture was centrifuged at 10,000 rpm for 25 min at 4 °C. The supernatant was added to separate tubes along with phosphate buffer (KH$_2$PO$_4$, K$_2$HPO$_4$) (pH 7.3), 1 mM EDTA, 0.5 Mm of Ascorbate, and 3 mM of H$_2$O$_2$. The decrease in ascorbate concentration was measured by taking the absorbance at 290 nm for 3 min at 3 s time intervals (E = 2.8 mM^{-1} cm^{-1}).

Isozymes (native PAGE method-SDS independent) of SOD, CAT, and APX were identified with the procedure of Shah and Nahakpam [50] with a few minor modifications.

For the analysis of SOD isozymes [51], 500 mg leaf samples were homogenized with 1 mL of extraction buffer (pH 7.8) containing 100 mM of potassium phosphate buffer (K$_2$HPO$_4$; KH$_2$PO$_4$), 1 mM of EDTA, 3 mM of DL-Dithiothreitol (DTT) and 5% of PVP. The homogenized samples were further centrifuged at 10,500 rpm for 30 min at the supernatant was the sample used to run the native gel. The samples from 10 am and 2 pm were taken, each in the ratio of 2:1 (same for CAT and APX) of sample and dye (pH 6.8), which contained 240 mM of Tris-HCl, 40% of glycerol and 5% of bromophenol blue in 10% and 4% of resolving/separating and stacking buffer, respectively. The electrode buffer (pH 8.3) containing 25 mM of Tris-base and 192 mM of glycine was maintained at 4 °C at 80 V for about 3–4 h. The gel was further stained using staining solution [52] containing 50 mM of KH$_2$PO$_4$ AND K$_2$HPO$_4$ phosphate buffer, 1 mM of EDTA, 33.2 μm of riboflavin, 0.2% of TEMED and 0.245 mM NBT for 30 min. The gel was then irradiated in light for about 5 min in distilled water. Soon after the bands were visible, the distilled water was discarded and the gel was placed in 6% acetic acid to terminate the reaction. The bands with isoforms were further visualized under a trans-illuminator.

For CAT isozymes [53], the sample volume and extraction buffer were the same as used in the SOD analysis. The gel percentage was also the same at 10% and 4%. After the gel was run (similar to SOD), it was further immersed in distilled water containing 0.003% hydrogen peroxide (H$_2$O$_2$) for 10 min. The solution was then discarded and the gel was washed gently with distilled water for 2–3 s. The gel was then stained using a staining solution [54] containing 0.5% potassium ferrocyanide (K$_3$Fe(CN)$_6$) and 0.5% ferric chloride (FeCl$_3$) for about 10 min. Then, again the staining solution was discarded and the gel was gently washed with distilled water a single time. The gel containing CAT isoforms was visualized under a trans-illuminator.

For the APX isozymes analysis [55], 200 mg of leaf material was homogenized with 2 mL of extraction buffer (pH 7.8) containing 50 mM of potassium phosphate buffer (K$_2$HPO$_4$; KH$_2$PO$_4$), 1 mM of EDTA, 1 mM of phenyl methyl sulfonyl fluoride (PMSF-dissolved in 1 mL of ethanol), 5 mM of ascorbate and 2% of PVP. The homogenized samples were centrifuged at 15,000 rpm for 10 min. The gel percentage remained the same as in the SOD analysis with an electrode buffer (pH 8.3) containing 0.1 M of Tris-base and glycine. After running the sample in gel [56], it was equilibrated with a solution containing 50 mM

of potassium phosphate buffer (pH 7.0) and 2 mM ascorbate for about 30 min. Then the gel was incubated with 50 mM potassium phosphate buffer (pH 7.0), 4 mM of ascorbate and 2 mM of H_2O_2 for 20 min (incubation was started as soon as H_2O_2 was added). The gel was further washed with 50 mM potassium phosphate buffer (pH 7.0) for 1 min. The gel was then submerged in the staining solution containing 50 mM potassium phosphate buffer (pH 7.8), 28 mM TEMED and 2.45 mM NBT with gentle agitation. The gel appeared purple-blue in color and the APX isoforms were observed within 3 to 5 min.

2.9. Stomatal Index and Structure

To investigate the stomata [57], a small thin epidermal (outer) layer of leaf tissue was peeled out gently. The peel was carefully placed on a glass slide, a few drops of water were added, and a cover slip was placed on top. The structure of stomata was observed under $10\times$ magnification and the stomatal index was observed using $40\times$ magnifications under a microscope (MEIJI TECHNO CO., LTD., Kyoto, Japan). The stomatal index was calculated by dividing the number of stomata by ten times the area of one square grid. Basically, the stomatal index is, in a unit area of a leaf sample, the percentage of the total number of stomata to the total number of epidermal cells.

2.10. Protein Analysis

To estimate the total protein content present in the samples, 0.2 g of leaf samples were taken and homogenized using the extraction buffer (pH 7.0) containing 1 mL of 0.2 M phosphate buffer, 2% PVP, 0.5% of Triton-X 100 and 1 mM EDTA. Soon after the extraction, it was centrifuged at 12,000 rpm for 20 min at 4 °C. The supernatant was used for the quick analysis of protein by the Bradford method [58] using bovine serum albumin (BSA) as a standard. The absorbance of total protein content present in the extracted enzyme samples was measured at 595 nm using a UV-Spectrophotometer.

The relative total protein profile was first evaluated in the first dimension using sodium dodecyl polyacrylamide gel electrophoresis (SDS-PAGE) [59]. The plant samples were ground to fine powder using liquid nitrogen. The extraction of protein was performed using extraction buffer [60] containing 40 mM (*w/v*) Tris-HCl (pH 7.5), 2 mM (*w/v*) EDTA, 0.07% (*w/v*) β-mercaptoethanol, 2% (*w/v*) PVP (polyvinylpyrrolidone) and 1% (*v/v*) Triton X-100, followed by centrifugation of the extracts at 13,000 g for 10 min at 4 °C. 6X protein-dye containing 240 mM Tris-HCl (pH 6.8), 40% glycerol, 8% SDS, 0.04% bromophenol blue and 5% beta-mercaptoethanol was mixed with the extract obtained after centrifugation. Quantification of protein samples was performed using the Bradford assay, and the standard curve was plotted using BSA (bovine serum albumin) [58]. The protein samples (25 μL) were loaded on 12.5% polyacrylamide gel on PROTEAN II (Bio-Rad, Hercules, CA, USA) and the gel was run in the range of 60 V to 100 V and stained later using Coomassie brilliant blue (CBB stain).

2.11. Analysis of Native Protein in Thylakoids by 1D BN-PAGE

Fresh leaves were collected from the plants and a first dimension BN-PAGE of integral thylakoid proteins was performed according to previous studies [61]. The leaves were washed carefully with distilled water and immediately ground to fine powder in a pestle and mortar using liquid nitrogen. Around 5 g of powdered samples was homogenized in pre-chilled buffer (PH 7.8) containing of mixture of 330 mM sorbitol, 2 mM EDTA, 50 mM HEPES, 2 mM Na, and 5 mM $MgCl_2$. The mixture was filtered via Mira cloth. Centrifugation was performed at $4500\times g$ for 10 min at 4 °C, and the pellets obtained were re-suspended in the same ice-cold buffer. Again, centrifugation was performed as in the first step. Subsequently, another buffer containing 20 mM tricine, 70 mM sucrose, and 5 mM $MgCl_2$ (pH 7.8) was used, and the pellet obtained above was suspended again followed by centrifugation at $4500\times g$ for 10 min at 4 degrees. After that, washing of the final pellet was performed twice for approximately 2 min each using the washing buffer (330 mM sorbitol, 50 mM BisTris-HCl (pH 7.0) and 0.1 mgml-1 pefabloc) to obtain a purified protein pellet.

The final pellet obtained after washing was dissolved carefully in 2% *w/v* n-dodecyl-ß-D-maltoside for solubilization and further mixed with 0.1% loading dye (5% CBB-G250, 100 mM BisTris-HCl (pH 7.0), 30% *w/v* sucrose and 500 mM ε-amino-n-caproic acid). The protein samples extracted from the above steps were loaded on 5–12% *w/v* acrylamide gradient gel (1.5 mm). The Bradford assay was used to determine the protein concentration. First dimension BN-PAGE was performed by running the gel electrophoresis at 4 °C in a Protean II xi Cell electrophoresis system (Bio-Rad, Hercules, CA, USA) at a constant voltage of 100 volts for 5–6 h until the gel run was complete.

2.12. Statistical Analysis

A completely randomized design was used with three biological replicates for all treatments. An individual Student's t-test and Tukey's test were employed to compare the means of separate replicates using software SAS (version 9.1, Cary, NC, USA).

3. Results

3.1. Plant Height and Leaf Appearance

It was observed that the salt-treated plants had a significant decrease in height with increase in salinity stress compared with control plants. In MJ (Malav Jyoti), on day 5 of treatments, control (untreated) plants were healthy and taller compared with the salt-treated plants; similarly, in DG (Delhi Green), the control plants were taller than the stressed plants. However, at day 10 of salinity stress, in MJ, the control plants appeared shorter than the treated plants. In contrast, in DG, the control plants were still taller than the treated plants (Figure 1). There were no large differences observed for T2, T3 and T6, whereas T1, T4 and T5 showed substantial variance. The leaves of MJ were broad and light green in appearance at day 5, and it was similar in DG at day 10. However, the leaves of MJ at day 10 and DG at day 5 appeared small and dark green in color (Figure 1). The plant height was analyzed based on three biological replicates for each set of samples, for example, by collecting three different plants from three different grow bags.
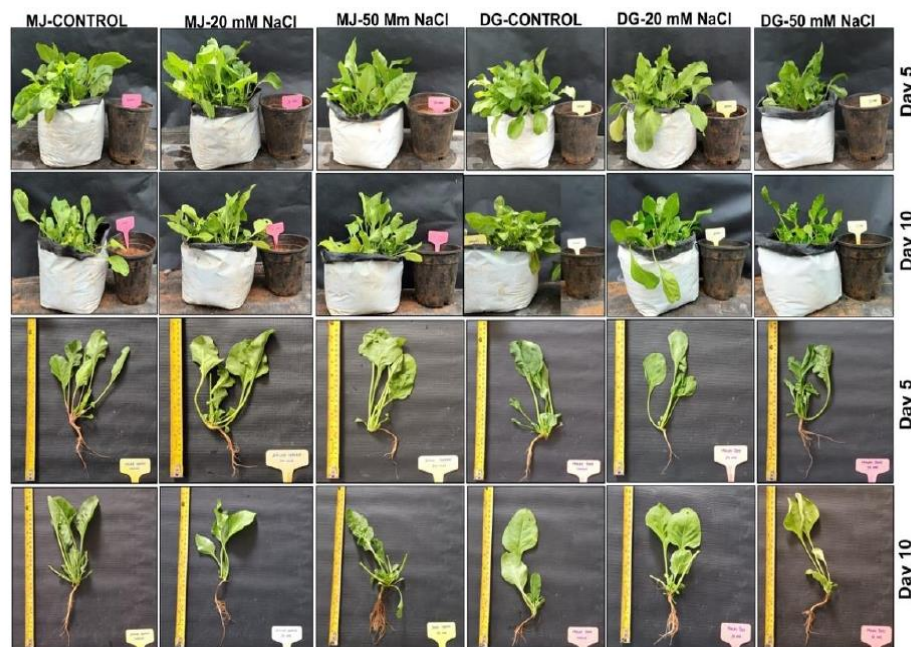

Figure 1. Morphological appearance of spinach genotypes Delhi green (DG) and Malav Jyoti (MJ). Each grow bag represents approximately 6 to 8 seeds sown, which went through a further thinning process. For each genotype, 15 grow bags were separated into 3 groups: 5 bags for control, 5 bags for the 20 mM of NaCl treatment, and 5 bags for the 50 mM of NaCl treatment. The leaf samples were collected between at time intervals (on the basis of circadian cycle) of about 4 h, which were at the exact times of 6 am, 10 am, 2 pm and 6 pm on day 5 and day 10 of the salinity stress treatments.

3.2. Root Length and Appearance

The increase in salt stress showed a significant decrease in root length for both MJ and DG genotypes. At day 5 of salt treatment, in MJ, it was observed that the T2 and T3 plants had a significant reduction compared with the T1 plants. Similarly, in DG, the T5 and T6 plants had a significant increase in plant height compared with the T4 plants (Figure 2A). At day 10, there was an increase in root length observed in MJ plants, whereas in DG, the root lengths of plants remained almost constant in T5 and T6 (Figure 2C), which was a reduction compared with T4. It was observed that the roots appeared in a tap root structure at day 5; whereas at day 10, the plants had a fibrous root structure, which was clearly evident in T3 and T5 (Figure 1). As mentioned for plant height, the root lengths of three different plants were measured as biological replicates of each sample.
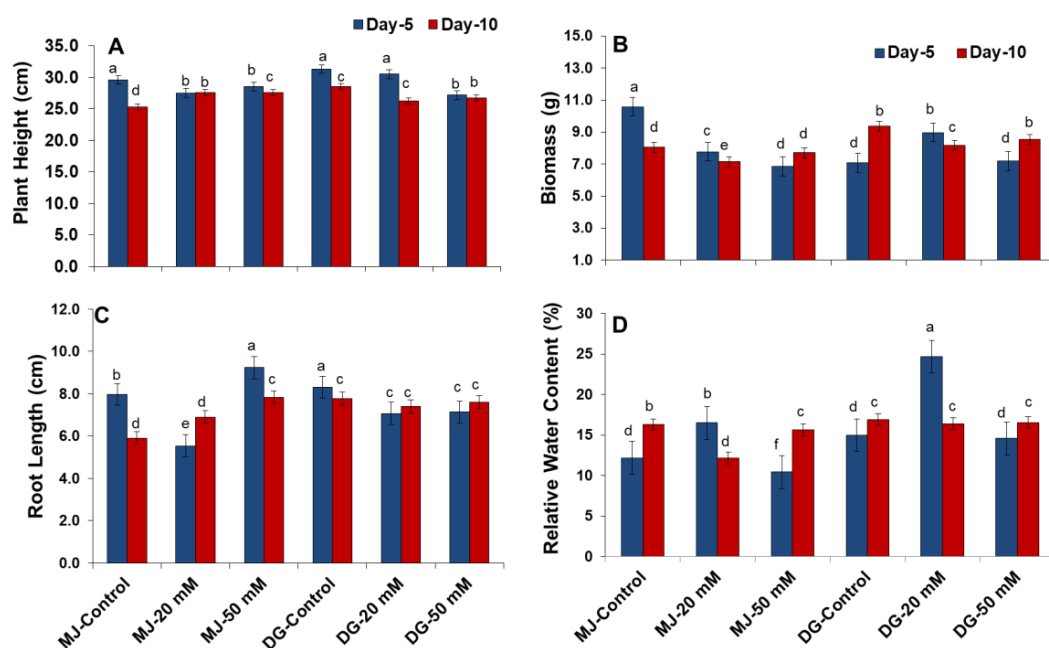

Figure 2. (**A**) Plant height, (**B**) biomass, (**C**) root length, and (**D**) relative water content in spinach genotypes Delhi green (DG) and Malav Jyoti (MJ). Results are presented for the controls (MJ control; DG control), 20 mM of NaCl treatments (MJ-20 mM; DG-20 mM), and 50 mM of NaCl treatments (MJ-50 mM; DG-50 mM). Vertical bars indicate mean $\pm$ S.E. for $n = 3$. Means with different letters are significantly different at $p \leq 0.05$ according to the Tukey's studentized range test. The blue color bars indicate the day 5 results and the red color bars indicate the day 10 results.

3.3. Biomass and Relative Water Content

Biomass at day 5 showed a significant decrease with increase in salt concentration in the MJ genotype. The T1 (control) plants appeared to have an increased level of biomass compared with T2 (MJ-20 mM) and T3 (MJ-50 mM) plants (Figure 2B), whereas in the DG genotype, there was a significant increase observed with increasing minimum salt conditions (T5) compared with T4 (control) and high salt condition (T6). At day 10, there was a significant decrease observed in T2 and T3 spinach plants compared with the T1 plants. Similarly, there was a significant decrease in T5 and T6 spinach plants compared with the T4 plants.

Considering the relative water content of leaves, there was a peak in minimum salt treated plants at day 5 in both spinach genotypes, whereas the same T2 and T4 treatments showed a significant reduction in RWC by day 10 (Figure 2D). It was observed that an increase in salt concentration had a negative effect on RWC; thus, there was a reduction in T2 plants at day 5 in MJ compared with T1 and T3 plants. Similarly, in DG, at day 5 (early stress state), the T5 plants has showed a peak. At day 10, the T1 plants showed an increase in RWC compared with the T2 and T3 plants, and the same observation was made for the DG plants.

3.4. Malonaldehyde (MDA) and Proline Content

At 6 am of day 5, the MDA content was at a peak; at 10 am, the level of MDA was less, but at 2 pm it had again increased and by 6 pm, it had reduced (Figure 3A). At 10 am of day 10, the MDA level was high; again at 10 am, it was at a peak, whereas at 2 pm and 6 pm, a significant reduction in MDA content was observed. However, if we compare the circadian timings with salt stress, it is found that on day 5 at 6 am, the MDA contents in T2, T3, T5 and T6 were less than those in T1 and T4. At 10 am, in T1 a significant increase was observed compared with both stress concentrations T2 and T3, whereas in DG, the increased stress volume (T6) showed a significant increase in MDA content. At 2 pm, the pattern was similar to the 10 am samples where the control was at a comparative peak. At 6 pm, in MJ, the stress treatment (T3) showed an increase in MDA content, but in T4, a higher peak was observed than in the T5 and T6 plants. On day 10 at 6 am, T2 and T5 showed a peak compared with T1, T4, T3 and T6. At 10 am, T1 showed an increase in MDA content compared with T2 and T3, whereas in DG, the increased stress treatment (T6) showed a significant increase in MDA content. At 2 pm, there was a comparative increase in MDA in T2 and T5. At 6 pm, it was again similar to the 10 am and 2 pm levels of day 10 in the MJ plants, but in the DG plants, there was an increase in the MDA levels in the T4 plants compared with the T5 and T6 plants. Overall, significant increases in MDA content were observed at 10 am and 2 pm that correspond to rhythmic circadian loop cycles under salinity stress conditions, which suggests a contribution of the circadian clock to the alleviation of salinity stress. Moreover, the DG genotype was observed to be more tolerant towards salinity stress and associated with circadian biology.
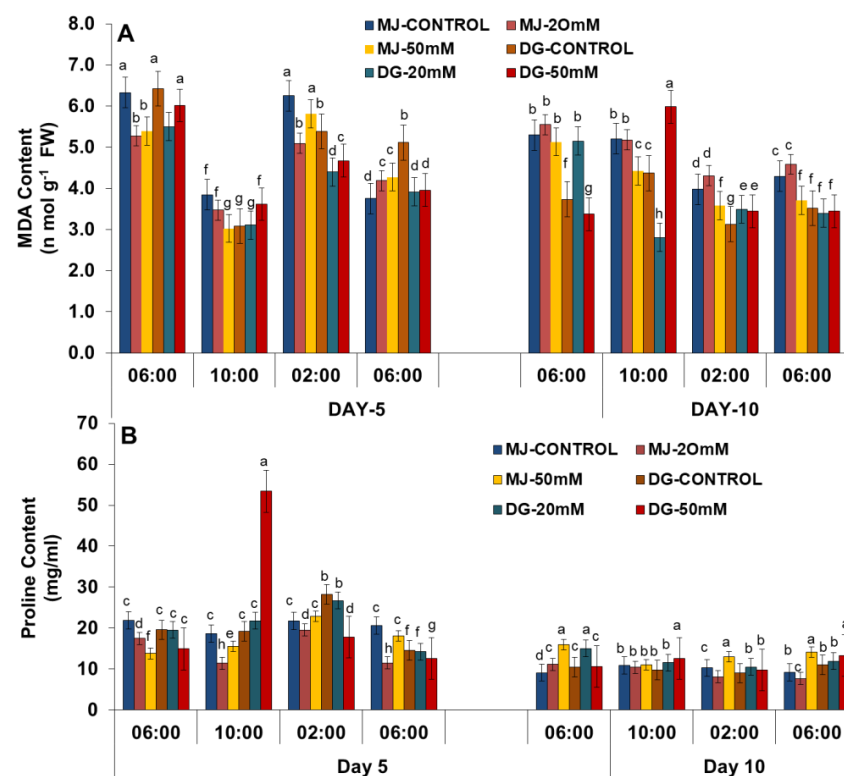

Figure 3. (**A**) MDA content and (**B**) proline content in spinach genotypes Delhi green (DG) and Malav Jyoti (MJ). Results are presented for the controls (MJ control; DG control), 20 mM of NaCl treatments (MJ-20 mM; DG-20 mM), and 50 mM of NaCl treatments (MJ-50 mM; DG-50 mM). Sampling was performed (on the basis of circadian cycle) at 4 h intervals which were at 6 am, 10 am, 2 pm and 6 pm on both day 5 and day 10 of salinity stress. Vertical bars indicate mean ± S.E. for $n = 3$. Means with different letters are significantly different at $p \leq 0.05$ according to the Tukey's studentized range test. Data for day 5 and day 10 are shown separately and the colors of the bars correspond to treatments, which remain the same for different hours.

Proline is a stress indicator; thus, an increase in proline content in plant samples indicates an increase in the presence of stress. On day 5 at 6 am, the proline content appeared to be less but at 10 am, it was increased (Figure 3B). Similarly, at 2 pm there was a peak, but at 6 pm there was a significant reduction in proline content. On day 10, the proline content was less compared with day 5 at all circadian hours. However, there was a significant increase observed in proline content, on day 10 at all circadian hours and also in all stressed samples compared with the control samples.

3.5. H_2O_2 and O_2^- Localization

The increase in LPO or MDA content can lead to increases in the ROS accumulation in the form of H_2O_2 and O_2^-. With help of biochemical analysis, it was found that the DAB (H_2O_2) test results in dark brown color spots on leaf samples and that the NBT (O_2^-) test shows dark blue (formazon formation) color spots on the leaf samples (Figures 4 and 5). The hydrogen peroxide localization is consistent with the fact that the increase in salt concentration in plants leads to an increase in localization of H_2O_2, with an increase in the days of salt treatment.
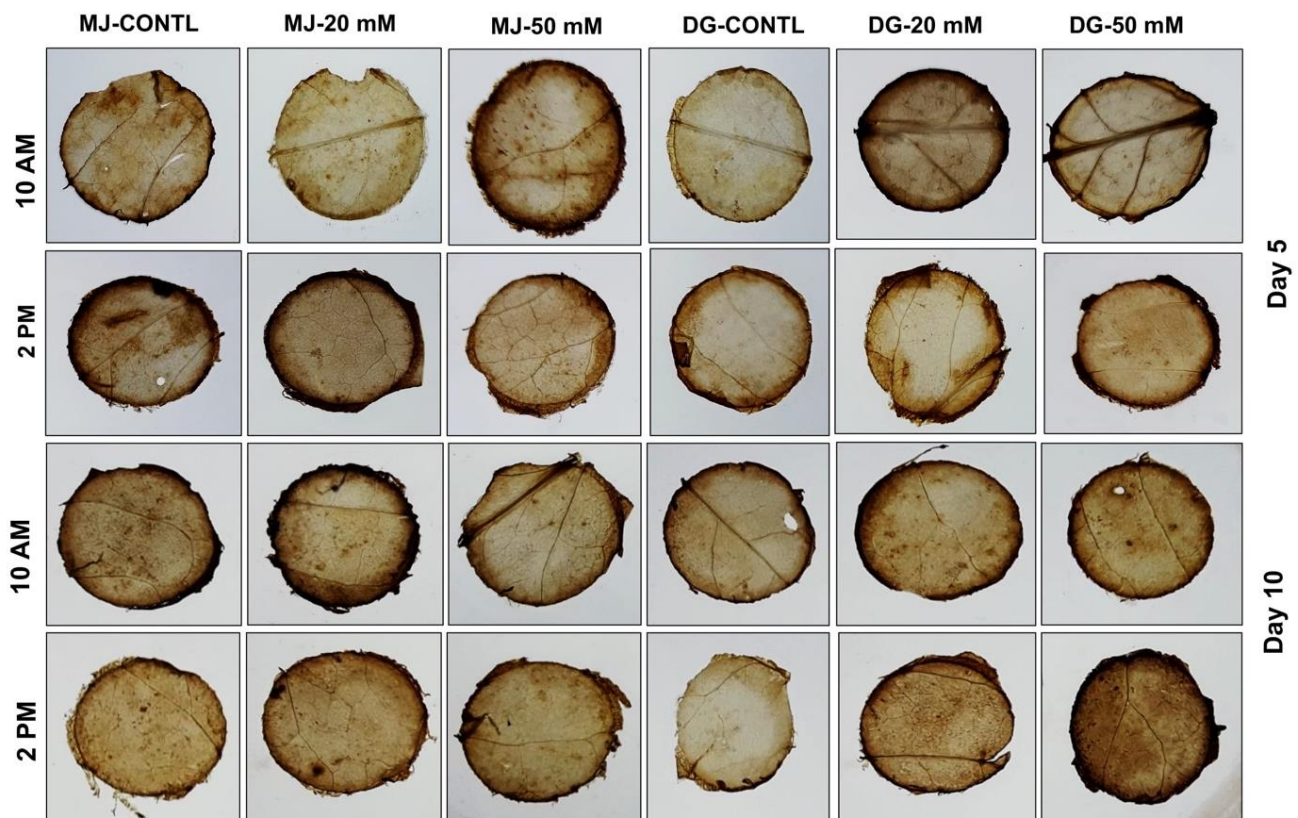

Figure 4. H_2O_2 localizations in spinach genotypes Delhi green (DG) and Malav Jyoti (MJ). Images are presented for the controls (MJ control; DG control), 20 mM of NaCl treatments (MJ-20 mM; DG-20 mM), and 50 mM of NaCl treatments (MJ-50 mM; DG-50 mM). Sampling was performed (on the basis of the circadian cycle) at 4 h intervals which were exactly at the times of 10 am and 2 pm on both day 5 and day 10 of the salinity stress treatments.

For the physiological parameters and enzymatic activities, 4 h intervals corresponding to circadian hours were chosen for prediction of ROS generation in spinach plant samples. At day 10 of salt stress, the treated leaf samples showed an increase in dark brown spots in both spinach genotypes compared with day 5 of the treatment. Considering the H_2O_2 localization results, on day 5 at 10 am, T3, T5 and T6 had an increase in brown spots, and in the 2 pm leaves, T2 and T6 showed more spots, whereas on day 10 at 10 am, for T2,

T3, T5 and T6, increased spots were noted, and this was the same at 2 pm of day 10. The superoxide radical localization also showed that the increase in salt stress leads an increase in the $O_2{}^-$ localization. On day 5, at 10 am, the T3 and T5 samples had comparatively high localized $O_2{}^-$, whereas in the 2 pm samples, T2, T3 and T6 showed a better result. On day 10 at 10 am, there was significant increase in T3, T5 and T6 leaves, whereas at 2 pm, T2 and T5 had a significant increase.
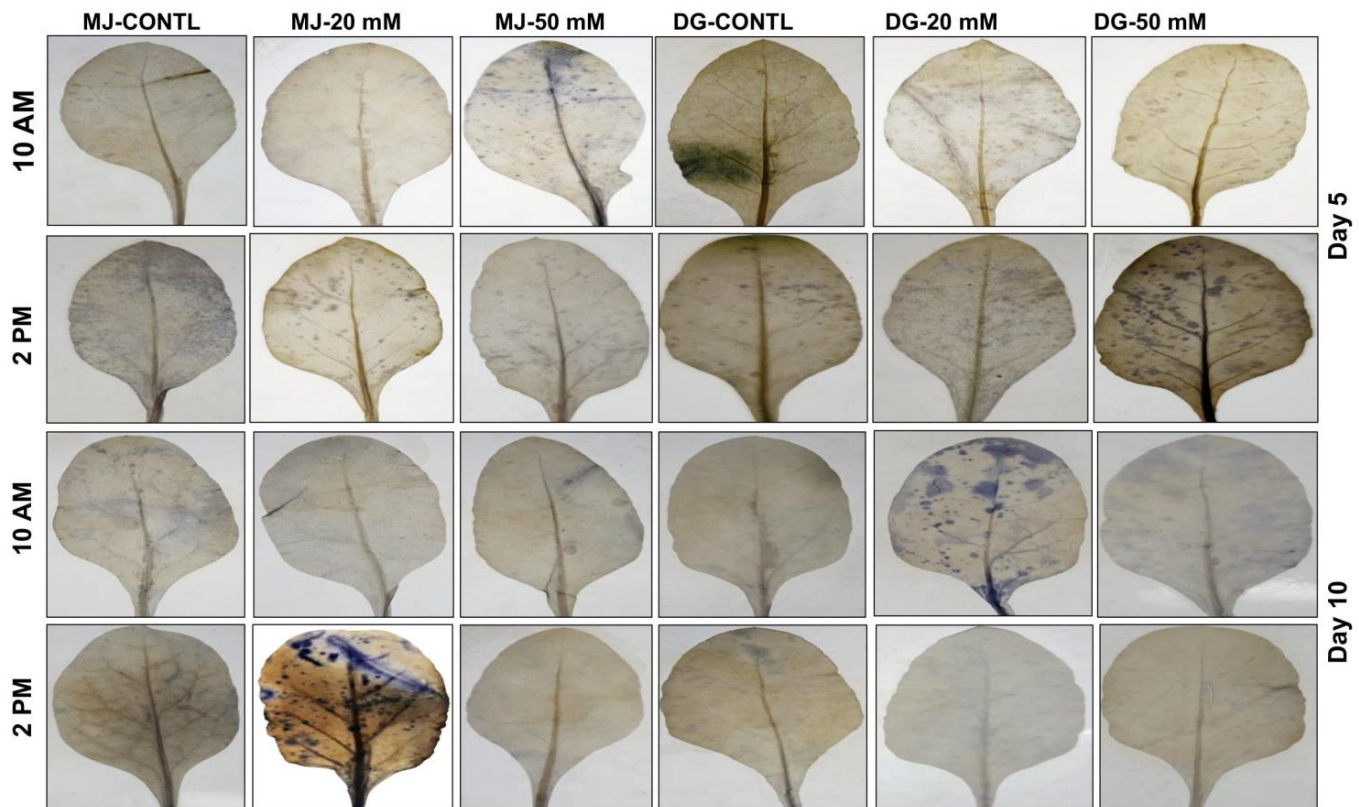

Figure 5. $O_2{}^{-1}$ localizations in spinach genotypes Delhi green (DG) and Malav Jyoti (MJ). Images are presented for the controls (MJ control; DG control), 20 mM of NaCl treatments (MJ-20 mM; DG-20 mM), and 50 mM of NaCl treatments (MJ-50 mM; DG-50 mM). Sampling was performed (on the basis of the circadian cycle) at 4 h intervals corresponding to the times of 10 am and 2 pm on both day 5 and day 10 of salinity stress.

3.6. Photosynthetic Measurements

A significant decrease in the net photosynthesis rate with increasing salt concentration was reported. On day 5 at 6 am, the rate of photosynthesis was less, whereas at 10 am and 2 pm, it was at its peak, and again by 6 pm, it had reduced (Figure 6). A similar pattern was observed on day 10. However, at 10 am on day 5, T3 showed a contrary result compared with the other circadian hours with a significant decrease in T2 and T3. T5 also showed a contrary result at all circadian hours, whereas T6 showed significant decrease at all circadian hours of day 5. On day 10 at 6 am, there was a contrary result observed for T2, and similar to 2 pm, there was an increase in T3. Apart from that, there was a significant decrease at all circadian hours for both genotypes in salt-treated plant samples. The stomatal conductance and the transpiration rate also showed patterns similar to those for the net photosynthetic rate.
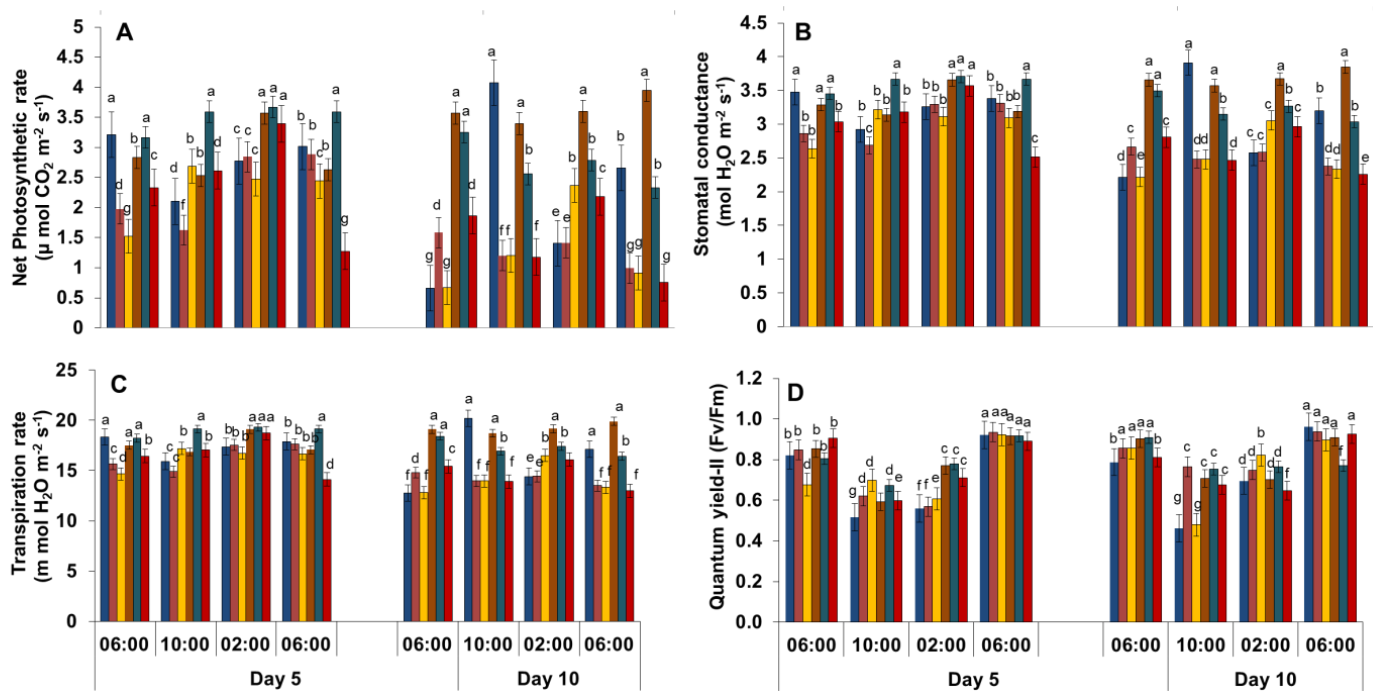
Figure 6. (**A**) Net photosynthetic rate, (**B**) stomatal conductance, (**C**) transpiration rate, and (**D**) PSII-quantum yield in spinach genotypes Delhi green (DG) and Malav Jyoti (MJ). Results are presented for the controls (MJ control; DG control), 20 mM of NaCl treatments (MJ-20 mM; DG-20 mM), and 50 mM of NaCl treatments (MJ-50 mM; DG-50 mM). Sampling was performed (on the basis of the circadian cycle) at intervals of about 4 h which were at the exact times of 6 am, 10 am, 2 pm and 6 pm of both day 5 and day 10 of salinity stress. Vertical bars indicate mean ± S.E. for *n* = 3. Means with different letters are significantly different at *p* ≤ 0.05 according to the Tukey's studentized range test. Data for day 5 and day 10 are shown separately and the colors of the bars correspond to treatments, which remain the same for different hours.

The PS-II quantum yield (Fv/Fm) usually decreases with an increase in salt stress in plant samples. On days 5 and 10, at 6 am and 6 pm, the quantum yield-II was at a peak, whereas at 10 am and 2 pm, it was observed to be less (Figure 6D). However, there was a significant decrease observed for T6 at 10 am and 2 pm of day 5 and day 10. In contrast, T2, T3, and T5 showed an increased chlorophyll fluorescence. There was a significant decrease observed for T3 at 6 am of day 5 and 6 pm of day 10. Similarly, there was a significant decrease observed with T5 at 6 am of day 5 and 6 pm of day 10. Overall, the photosynthesis measurements showed that the circadian clock can help plants improve their response and withstand salinity stress at specific time periods such as 10 am and 2 pm.

3.7. Photosynthetic Pigments

The carotenoid and total chlorophyll content significantly decreased with increases in salt concentration in spinach plants (Figure 7). On day 5 at 6 am, the chlorophyll pigment content was less, whereas at 10 am and 2 pm, it was at a peak, and at 6 pm, it had reduced again. Day 10 had a similar pattern, but at 6 pm, the chlorophyll content increased. However, on day 5 at 6 am, T5 showed a significant decrease. At 10 am, T2 and T5 showed a significant decrease, and also at 2 pm, T3 showed a significant decrease. Significant reductions in photosynthetic pigments were observed on day 10 at 6 am for T2 and T5, at 10 am for T3, at 2 pm for T6, and at 6 pm for T2, T5 and T6.
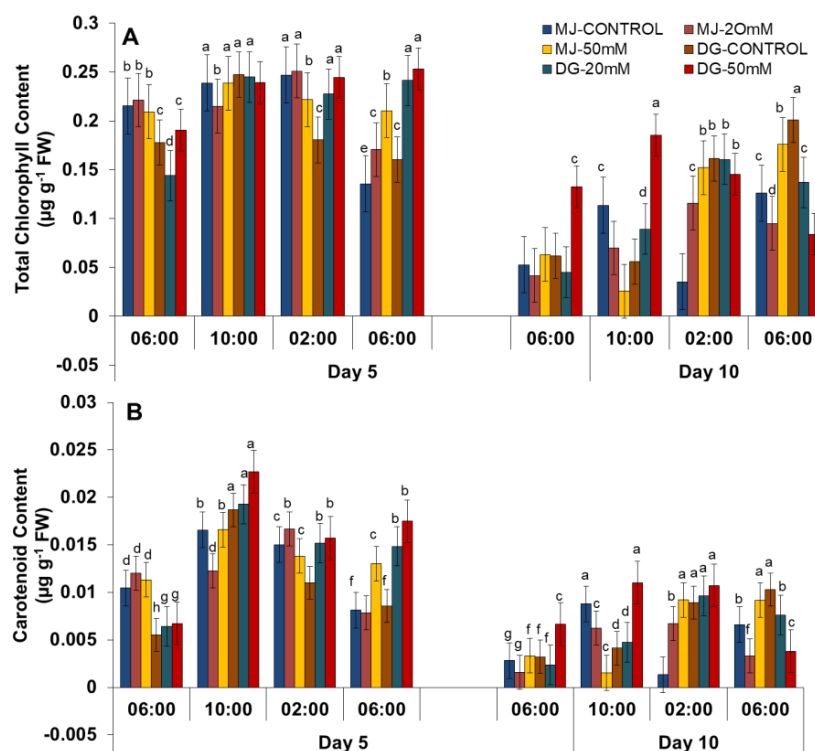
Figure 7. (**A**) Total chlorophyll and (**B**) carotenoid content in spinach genotypes Delhi green (DG) and Malav Jyoti (MJ). Results are presented for the controls (MJ control; DG control), 20 mM of NaCl treatments (MJ-20 mM; DG-20 mM), and 50 mM of NaCl treatments (MJ-50 mM; DG-50 mM). Sampling was performed (on the basis of the circadian cycle) at 4 h intervals which corresponded to the exact times of 6 am, 10 am, 2 pm and 6 pm on both day 5 and day 10 of salinity stress. Vertical bars indicate mean ± S.E. for *n* = 3. Means with different letters are significantly different at $p \leq 0.05$ according to the Tukey's studentized range test. Data for day 5 and day 10 are shown separately and the colors of the bars correspond to treatments, which remain the same for different hours.

3.8. Enzymatic Activities and Their Isozymes

The increase in salinity stress led to significant increases in the enzymatic activities (Figure 8). Except for SOD activity in DG in all photoperiodic hours, there was a significant increase in all stressed plant samples compared with the control plants. For APX activity, except in T3 at 6 am on day 5, there was significant increase at all circadian hours. Considering the CAT activity, in T2 at 10 am and in T3 at 2 pm and 6 pm, there was a significant increase with salt concentration compared with the control plants. This indicates that the MJ genotype was more tolerant of salt stress than DG.

An electrophoresis method was performed to obtain more comprehensive data on the isozymes of the major antioxidants (SOD, APX and CAT) at 10 am and 2 pm on day 10 (Figure 9). For SOD, there were two bands visualized in the UV-trans illuminator, which were indicated in both photoperiodic hours. In the 10 am samples for T2, it was highly expressed, and a prominent band was observed compared with other samples. This was followed by T3, which had greater expression than in T1 but less prominent than in T2. For DG, T4 and T6 had prominent bands compared with T5. At 2 pm, T3 and T6 had comparatively prominent bands. For APX, there were three different bands visible at both 10 am and 6 pm on day 10. At 10 am, T3 and T5 showed a prominent band where two were highly prominent and one band was slightly less visible in the image. There was a similar pattern found at 2 pm on day 10. For CAT, at 10 am on day 10, the T3 and T6 samples had prominent bands. The T2 and T5 bands were less prominent compared with T1 and T4. In contrast, at 2 pm, the T3, T5 and T6 samples had prominent bands, and T2 was less prominent compared with the T1 and T4 samples. The overall observations from enzymatic antioxidants and their isozymes indicate a large contribution of the circadian clock to tolerating salinity stress.
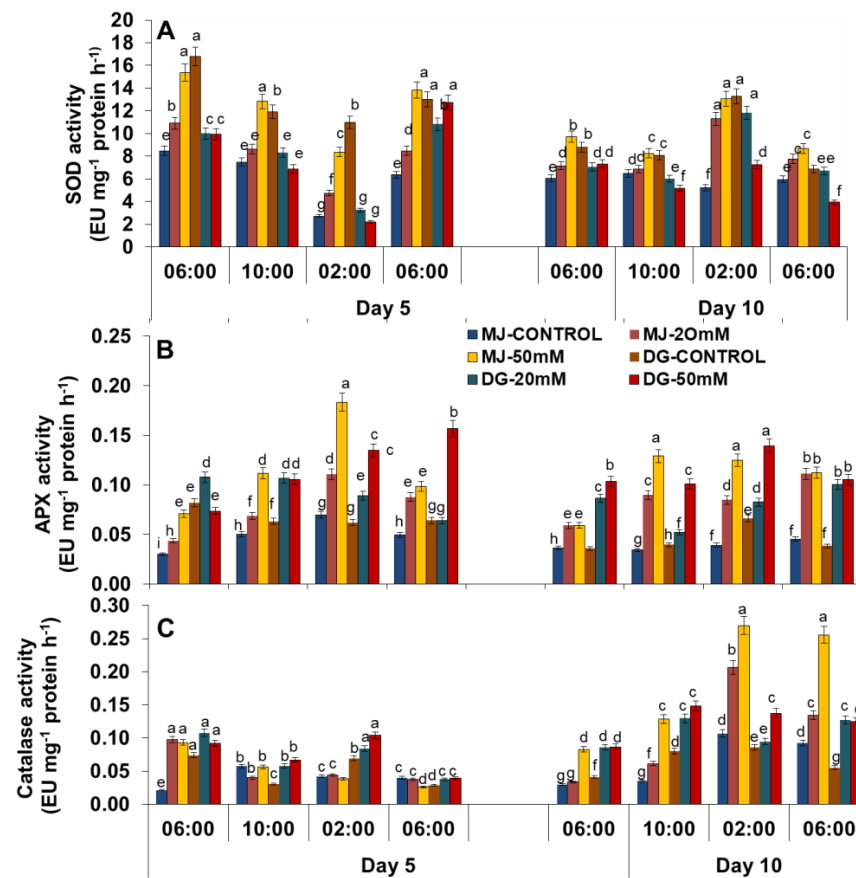
Figure 8. (**A**) SOD, (**B**) APX, and (**C**) catalase activity in spinach genotypes Delhi green (DG) and Malav Jyoti (MJ). Results are presented for controls (MJ control; DG control), 20 mM of NaCl treatments (MJ-20 mM; DG-20 mM), and 50 mM of NaCl treatments (MJ-50 mM; DG-50 mM). Sampling was performed (on the basis of the circadian cycle) at 4 h intervals corresponding to the exact times of 6 am, 10 am, 2 pm and 6 pm on both day 5 and day 10 of salinity stress. Vertical bars indicate th mean $\pm$ S.E. for n = 3. Means with different letters are significantly different at $p \leq 0.05$ according to the Tukey's studentized range test. Data for day 5 and day 10 are shown separately and the colors of the bars correspond to treatments, which remain the same for different hours.
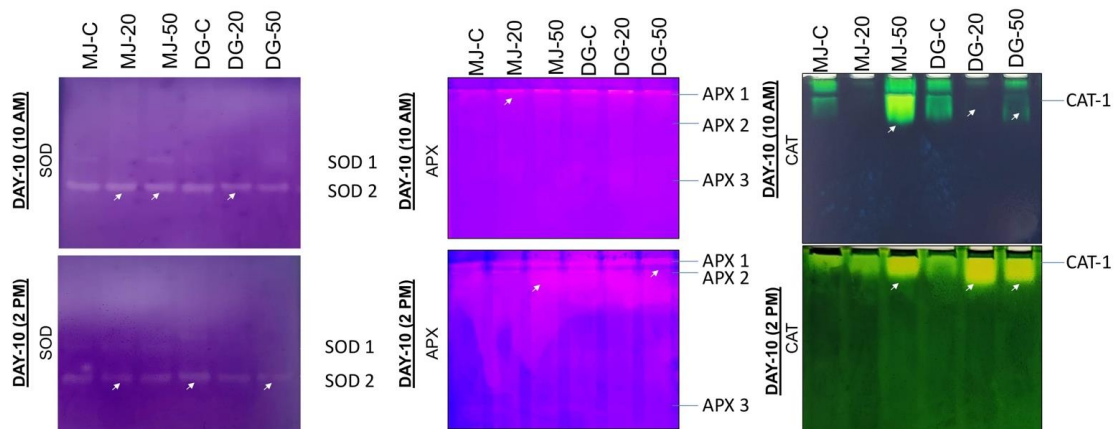

Figure 9. SOD, APX, and CAT isozyme activities in spinach genotypes Delhi green (DG) and Malav Jyoti (MJ). Results are presented for controls (MJ control; DG control), 20 mM of NaCl treatments (MJ-20 mM; DG-20 mM), and 50 mM of NaCl treatments (MJ-50 mM; DG-50 mM). Sampling was performed (on the basis of the circadian cycle) at 4 h intervals which corresponded to the exact times of 10 am, and 2 pm on day 10 of salinity stress. The white arrows indicate the changes in expression of bands among all treatments compared with controls.

3.9. Stomatal Index and Stomatal Structure

The increase in salt stress in the plant samples led to the closure of stomata (Figure 10A). On day 10 at 10 am, the T1 and T4 the stomata were seen to be open, whereas in T2 and T5 they were partially closed, and in T3 and T6, the stomata appeared fully closed. In contrast, at 2 pm on day 10, the T1 and T4 samples had partially open stomata, and the rest of the samples (T2, T3, T5 and T6) had closed stomatal structures.
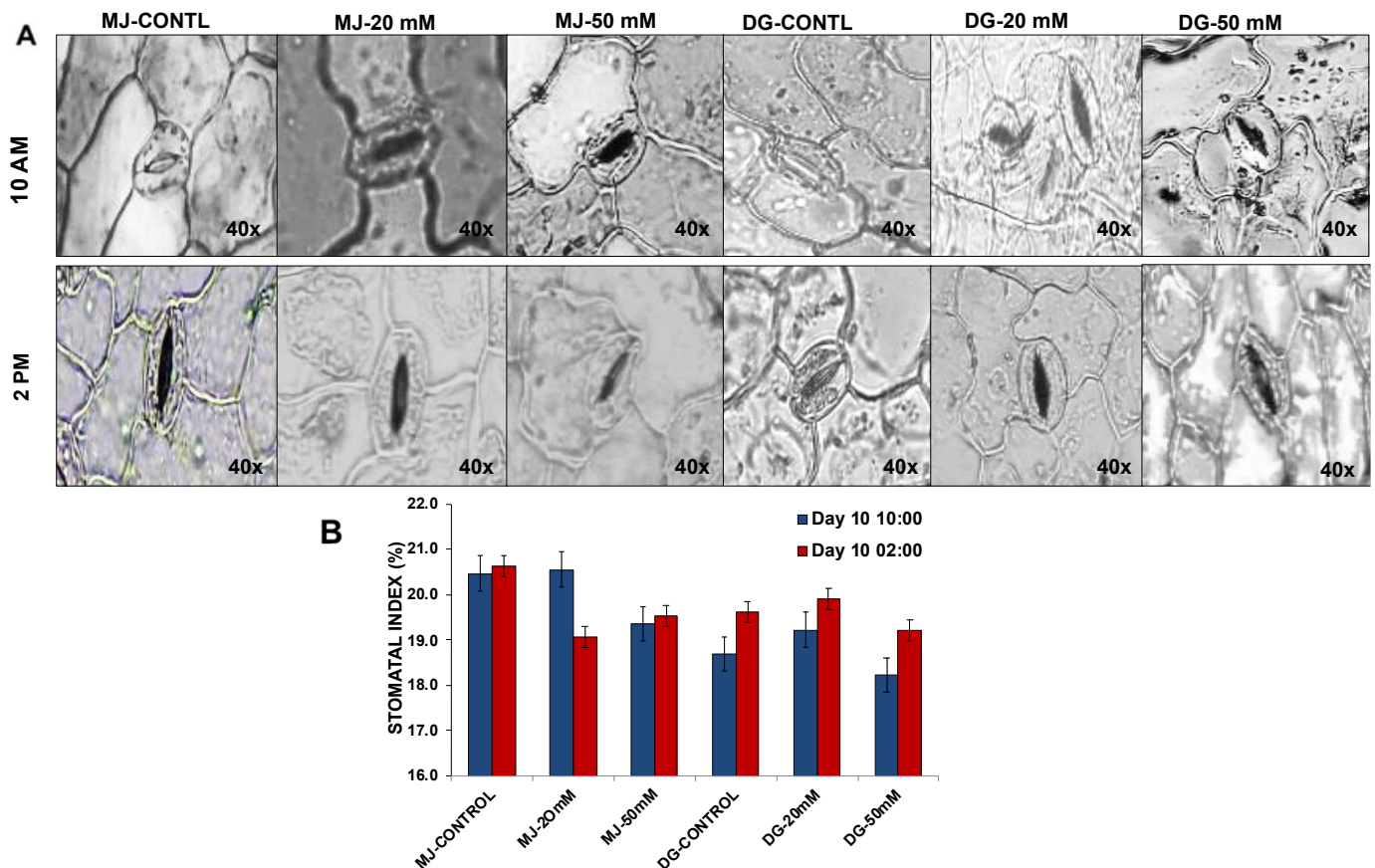

Figure 10. (**A**) Stomatal structure and (**B**) stomatal index in spinach genotypes Delhi green (DG) and Malav Jyoti (MJ). Results are presented for controls (MJ control; DG control), 20 mM of NaCl treatments (MJ-20 mM; DG-20 mM), and 50 mM of NaCl treatments (MJ-50 mM; DG-50 mM). Sampling was performed (on the basis of the circadian cycle) at 4 h intervals which corresponded to the exact times of 10 am, and 2 pm on day 10 of salinity stress. Vertical bars indicate mean ± S.E. for *n* = 3. The blue color bars in the graph indicate day 5 and the red color bars indicate day 10.

The increase in salt concentration led to a decrease in the number of stomata and an increase in the number of epidermal cells. On day 10, there was a significant decrease in T3 and T6 at 10 am, and at 2 pm, T2, T3 and T6 had the huge decrease observed. In addition, there was a contrary result observed for T2 and T5 at 10 am and also for T6 at 2 pm compared with the T1 and T4 (control) samples (Figure 10B).

3.10. Protein Analysis

The proteomic changes were analyzed using 1D SDS-PAGE to predict the enhancement of the protein for thylakoid protein analysis (Figure 11B). The bands were observed with either an upregulation or a downregulation of proteins for all spinach samples on the basis of the photoperiodic hours 10 am and 2 pm on day 10. The protein in the stressed plant samples had most of the proteins upregulated compared with the control samples. The only band that appeared more prominent and upregulated in all samples at both circadian hours was (Ribulose-1, 5-bisphosphate carboxylase/oxygenase) RuBisCo, which is known

as an abundant protein in plants. To estimate the protein concentration in all samples, a biochemical assay was performed, which showed a significant difference between the spinach samples (Figure 11A). The MJ plants showed an increase even after being treated with salt concentration, whereas DG showed a significant decrease in salt-treated plants compared with their control samples. Thus, this indicates that the DG plants remain sensitive compared with MJ plants (a resilient genotype) at both 10 am and 2 pm.
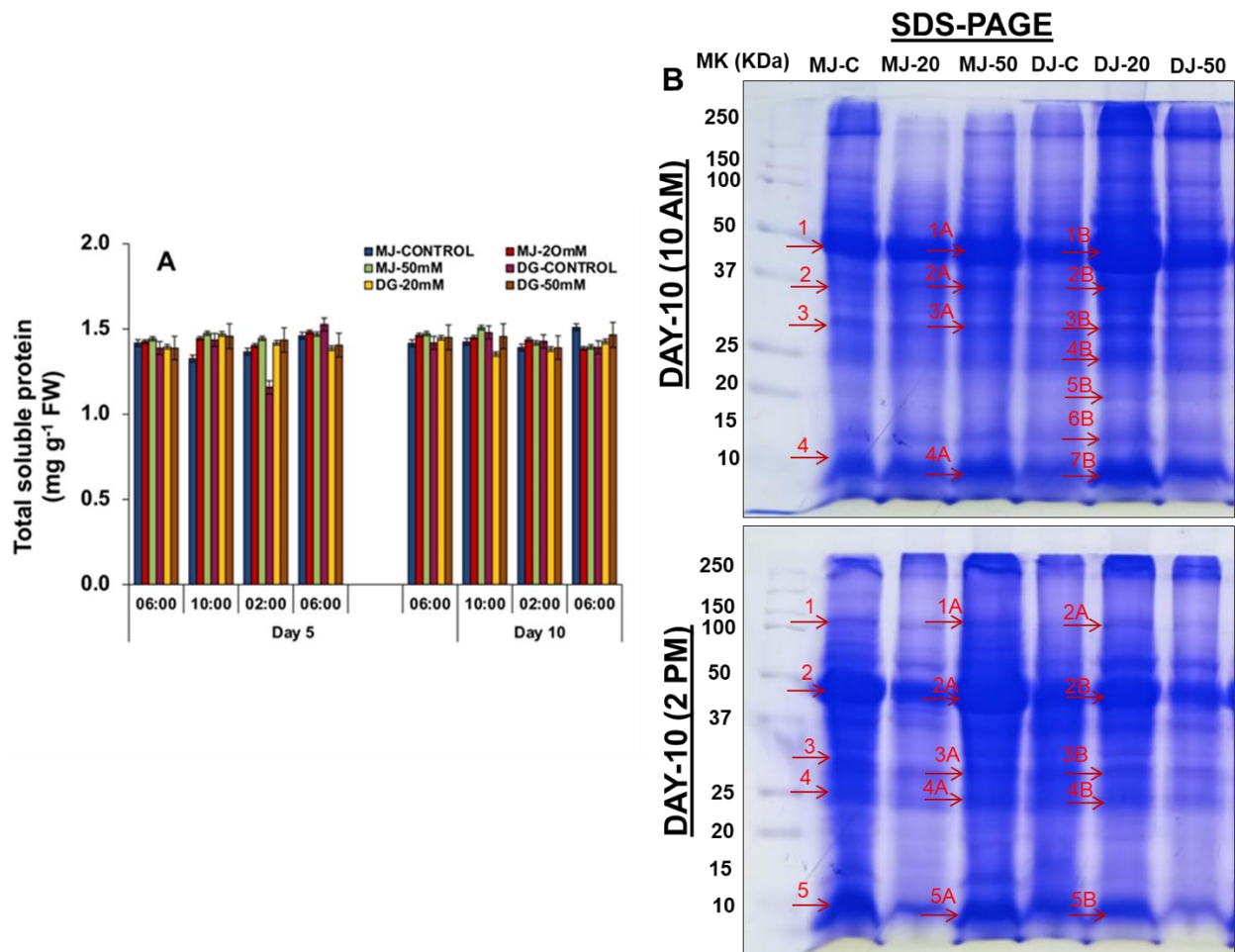

Figure 11. (**A**) Total soluble protein content, and (**B**) SDS-PAGE in spinach genotypes Delhi green (DG) and Malav Jyoti (MJ). Results are presented for the controls (MJ control; DG control), 20 mM of NaCl treatments (MJ-20 mM; DG-20 mM), and 50 mM of NaCl treatments (MJ-50 mM; DG-50 mM). Sampling was performed (on the basis of the circadian cycle) at 4 h intervals which corresponded to the exact times of 10 am, and 2 pm on day 10 of salinity stress. Vertical bars indicate the mean ± S.E. for *n* = 3. In bar graph (A), days 5 and 10 are shown separately but colors of the bars containing same samples at different hours remain the same. The red arrows with numbers indicate the upregulation or downregulation of specific proteins bands along with their controls.

3.11. Thylakoid Proteome Analysis

The BN-PAGE (Blue Native Polyacrylamide Gel Electrophoresis) analysis was carried out to separate the MCPs (multi-protein complex proteins) from the thylakoids which were isolated from the spinach leaves. The spinach leaves were collected based upon the different treatment conditions and circadian hours in three biological replicates. Figure 12 shows the gels containing the native proteome profile of thylakoid MCPs extracted at 10am from the leaf samples under the various treatments, including T1 (MJ control), T2 (MJ + 20 mM of salt), T3 (MJ + 50 mM of salt), T4 (DG control), T5 (DG + 20 mM of salt)

and T6 (DG + 50 mM of salt). In the other set, the treatments remained constant but the circadian hour was 2 pm.
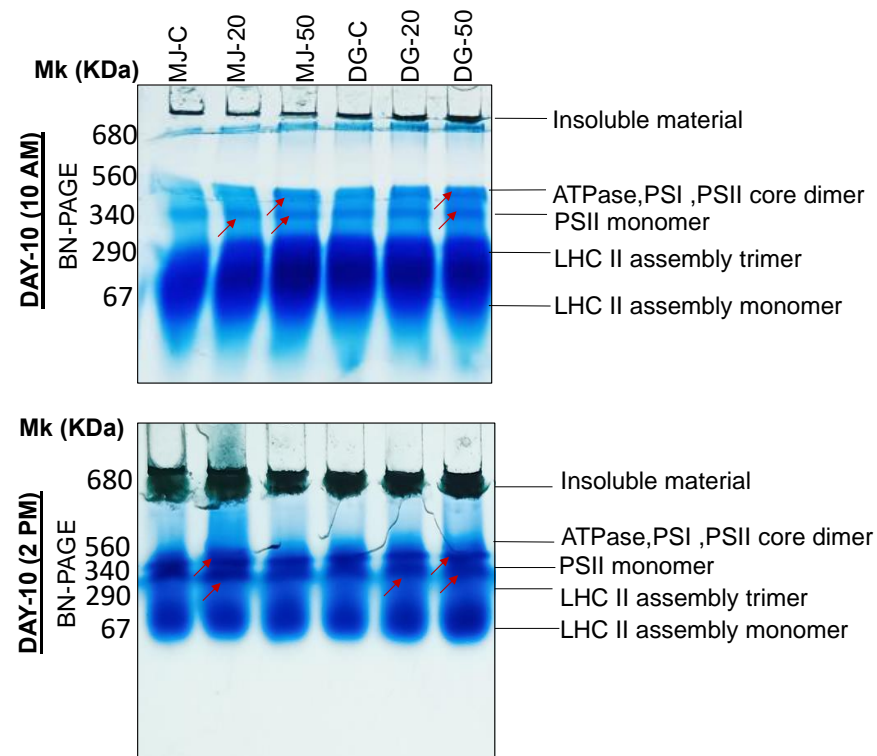

Figure 12. First dimension BN-PAGE in spinach genotypes Delhi green (DG) and Malav Jyoti (MJ). Results are presented for the controls (MJ control; DG control), 20 mM of NaCl treatments (MJ-20 mM; DG-20 mM), and 50 mM of NaCl treatments (MJ-50 mM; DG-50 mM). Sampling was performed (on the basis of the circadian cycle) at 4 h intervals which corresponded to the exact times of 10 am, and 2 pm of day 10 of salinity stress. For first dimension BN-PAGE, fresh thylakoid membranes of both spinach genotypes were solubilized in 1% BDM at a chlorophyll concentration of 1 $\mu g \cdot \mu L^{-1}$, and the protein sample was separated by 7%–12.5% gradient BN-PAGE. For second dimension gels, slices were horizontally laid on top of 12.5% SDS-PAGE and stained with a commercial Coomassie brilliant blue R-250 (Bio-Rad, Hercules, CA, USA). The arrows in the gel indicate the changes in expression of protein bands compared with their respective controls.

The expression of the very first protein band found in the gel was at 680–560 KDa, which is ATPase and PS-I, PS-II core dimer. The proteins in these bands were found to be downregulated with increasing salt stress in the leaf samples. The next consecutive band that appeared distinct was at 340 KDa, which was a PS-II monomer or Cyt b6/f. The last two bands were expressed in the ranges of 290 and 67, which are known as LHC-II assembly trimer and LHC-III assembly monomer, respectively. The bands of the MJ genotype were expressed slightly more distinctly, indicating that it can be a resilient or tolerant genotype towards salt stress under certain environmental conditions in various hours of the circadian rhythm. The BN-PAGE results were consistent with the results obtained for physiological mechanisms of photosynthesis.

4. Discussion

Circadian rhythms are important for a plant's daily activities whether it is flowering, fruiting, or any signaling pathways [62]. In recent years, it has also been observed that circadian rhythms are involved in the alleviation of abiotic stresses [63]. There are only reviews or limited studies reporting how circadian rhythms are involved in stress tolerance; therefore, the current study investigated how plants (spinach) tolerate stress, and salinity

in particular, using the circadian biological clock, especially during the morning–evening loop. Due to the toxic effects of Na^+ and Cl^- in the plant samples of our study (DG and MJ genotypes), there was a reduction observed in all growth parameters, whether it was plant height, biomass, or root length. The observed effects on relative leaf water potential were consistent with the measured growth parameters. Plants experience negative effects due to salt concentration which affect the plant's growth and performance. Plant biomass plays a vital role as an indicator of plant tolerance towards stress [64]. The increase in the uptake of salt was associated with a significant decrease in growth parameters, which is due to the formation of ROS (Figure 3) that, in turn, depress the ionic imbalance and plasma membrane. This leads to a suppression of metabolic processes and growth [65]. There was a similar result noted in a previous study with mung bean [18] subjected to salinity stress. The observed differences in root length of the plants may be due to the biological sample collection conducted to provide clarity.

Since this study focuses on how circadian biology time periods help the spinach plant to withstand the salinity stress, the main stress indicators, MDA and proline content, were focused on initially. Salt stress resulted in an increase in MDA content (an indicator of LPO) and proline content (an indicator of plant salinity response). For MDA, the increase in lipid peroxidation (MDA) indicates that LPO might exert its impact on lipid membrane permeability via the multiplication of micro viscosity, conceivably by way of a cross-linking process with lipid radicals, which contributes to the membrane damage that is generally linked with the leakage of ions. This then results in a decline in plant growth [66]. LPO increases due to the free radicals present in chloroplasts such as hydrogen peroxide, hydroxyl radicals and superoxide radicals. Considering proline, when the proline content increases, it tends to accumulate, which leads to further activity of a key enzyme (pyrroline-5-Carboxylate synthase) in the process of proline synthesis, along with the proline dehydrogenase enzyme inhibition which catalyzes proline degradation [67]. The plants receive protection from stress through controlling the osmo-regulation and through ROS detoxification. It also ensures preservation of membrane integrity, enzyme stabilization and certain other proteins [68,69]. However, in our results, a significant increase in MDA and proline content was observed at 10 am and 2 pm in the rhythmic cycle of the circadian loop (morning–evening loop) under salinity stress conditions, which suggests a contribution of the circadian clock in alleviation of salinity stress during this particular period of the circadian clock. It was also observed that the DG (Delhi green) genotype was more tolerant towards salinity and exhibited stronger circadian effects compared with MJ (Malav Jyoti).

It was observed that the stress markers MDA and proline content were significantly associated with oxidative damage in the spinach genotypes 'Delhi green' and 'Malav Jyoti' at specific photoperiodic times and circadian rhythms. Due to increase in salt concentration, ROS generation occurred in large amounts, which might result in membrane dysfunction, cell toxicity and cell death [70]. For scavenging the generated ROS, plants have developed various enzymatic and non-enzymatic mechanisms [71]. Due to salt stress, an oxidative burst takes place, which can be observed in the form of O_2^- and H_2O_2, and it was remarkably present in the leaf region of our spinach genotypes (DG and MJ) at the circadian times of 10 am and 2 pm (Figures 4 and 5). However, dramatic changes were observed compared with other circadian time periods in biochemically active stress markers, which indicates that the circadian clock can actively participate in tolerating salinity stress in spinach genotypes. To alleviate repair the damage due to the oxidative stress, plants have developed a complicated anti-oxidative system which comprises the SOD, APX, and CAT enzymes [72]. Our results showed a significant increase in enzymatic activities (except for SOD activity in DG) in all photoperiodic hours of circadian rhythms compared with the control plants (Figure 8). Moreover, MJ showed a better performance compared with DJ and indicated that the MJ genotype is more tolerant of salt stress than DG. Additionally, the circadian rhythms at a photoperiodic time of 10 am and 2 pm (morning–afternoon loop) showed a more tolerant timing. Therefore, based on the time period, we confirmed our antioxidant enzyme activities by their isozyme activities at 10 am and 2 pm of day 10 (Figure 9). The increase in

anti-oxidant enzymes under salt stress might help in protecting the chlorophyll content by preventing the leaf chlorophyll from becoming degraded. In addition, anti-oxidant enzymes are more effective in suppressing cell damage. In confirming the results with electrophoresis methods, the intensity of the bands had differences in most of the conditions rather than activation of new isoforms. From our antioxidant enzymes and their isozyme activities results, it was concluded that 10 am and 2 pm circadian rhythmic photoperiodism are the better time periods for tolerating salinity stress in spinach. It was also concluded that MJ is a more tolerant genotype through its use of circadian biology compared with DG. An analysis of the isozymes through native gel was performed to identify the isoforms of scavenging enzymes based on their size elution with the comparison of both genotypes, MJ and DG.

Photosynthesis is an integral mechanism of plant physiology, and due to salinity stress, all the photosynthetic measurements such as photosynthesis rate, stomatal conductance, and transpiration rate showed a significant reduction (Figure 6) at all circadian photoperiodic time periods, with less variation at 10 am and 2 pm. The decrease in these growth parameters could lead to further decreases in osmotic potential in soil. Under this condition, plants try to develop a mineral ion content and compatible solute production which combines soluble carbohydrates and proline [73]. This was similar to a previous study of salinity stress that examined stem and fruit samples of Japanese persimmon trees (*Diospyrus kaki* Thunb.) [74], where they also observed an increase in the sodium and potassium concentration, along with a reduction in water potential. Similar to our studies, a reduction was noticed in quantum yield-II, and chlorophyll pigments in mung bean [18]. The fluorescence in chlorophyll is an essential plant characteristic which shows the efficacy of the light reaction, and it is also used for understanding the effects of stress conditions on plants. The reduced level of chlorophyll fluorescence indicates the damage occurring in PS-II, which has major effects on the rate of photosynthesis. This results in a reduction in plant growth, development, and yield [75]. Consistent with results in tomato [76], a suppression of chlorophyll fluorescence under a constant light was observed, whereas the bean (*Phaseolus vulgaris*) [77] shows a reduction in photosynthesis and stomatal conductance under continuous light. The reduction in the stomata might be because the stomatal index is directly interlinked with the photosynthetic rate and growth parameters [63]. Since stomata are closely related to the transpiration rate and photosynthesis, it was observed that the changes in the structure of stomata and their index were particularly found at a photoperiodic time periods of 10 and 2 pm. The stomata were observed to be either partially or fully closed at noon time in our study (Figure 10). However, a contrary result was observed with *Phaseolus vulgaris L.* [76] where the plant samples at noon time showed the stomata opening. From our photosynthetic results and stomatal studies, it was concluded that spinach is able to tolerate salinity stress at a circadian time period of 10 am and 2 pm (morning–afternoon loop), which indicates that the circadian clock at certain photoperiodic time period influences the tolerance of salinity stress.

Our measurements of photosynthetic pigments, such as total chlorophyll content, were reduced significantly at all photoperiodic conditions, and less variation was observed at 10 am and 2 pm in the circadian cycle under salinity stress. The reduction in photosynthetic contents might be the result of an increased activity of chlorophyllase (chlorophyll degrading enzyme) [78,79]. The decreased chlorophyll content in salinity stress is mainly due to oxidative stress [80]. Similar results with chlorophyll content were observed in pumpkin genotypes [81], with *P. vulgaris L.* [82], and in *Vigna subterranean L.* [83]. The decrease in carotenoids was also observed under the salt stressed conditions in our study, but they increased significantly, even under salt stress, at 10 am in the circadian cycle. Carotenoids are anti-oxidants which have the ability to remove the toxic effect of ROS on plants [84]. They also function in photosynthesis to collect the light energy and as a quencher of tripled chlorophyll and oxygen [85].

The reduction in the photosynthetic rate was due to the reduction in leaf expansion, leaf senescence and improper functioning of the photosynthetic machinery [86]. To esti-

mate these effects in spinach genotypes, particularly at a circadian time period of 10 and 2 pm (morning–afternoon loop), a molecular level study, which was an effective tool for clear analyses, was chloroplast proteomics. A traditional gel electrophoresis (SDS-PAGE) (Figure 11) method found a reduction in RuBisCo protein at 2 pm in all samples compared with 10 am samples under salt stress. With the help of SDS-PAGE, either upregulation or downregulation of proteins with effective expressions were observed. The reason behind this might be the reduction in chlorophyll content and photosynthesis rate; this can also be due to variation in the structure of chloroplasts resulting from oxidative stress and reductions in protein synthesis [87]. The obtained results were confirmed by performing a biochemical analysis, which found a reduction in total protein under increased concentration of salt, with little variation observed in the 10 am and 2 pm circadian hour samples. Since the chloroplast is a major organelle involved in all biochemical processes, the proteome of the chloroplast was observed using blue native page at 10 am and 2 pm circadian hour samples. Many studies have previously reported the variation in the thylakoid proteome under salt stressed conditions, such as in tomato [62], mung bean [18], etc. However, it is not known how on the basis of circadian-based clock, the major photosynthetic proteins express themselves. There was a downregulation observed in the expression of thylakoid protein in salt stressed plants; in addition, there was decrease in the PS-I, PS-II monomer and LHC II assembly trimer protein complex, except for the LHC II assembly monomer observed at 10 am, which remained contrary in the 2 pm samples (Figure 12). These changes would have taken place due to the reduction in the photosynthetic and growth parameters in spinach genotypes, as observed previously in our biochemical processes of photosynthetic measurements.

Together with the obtained results at each circadian hour for stress indicators, photosynthetic parameters, photosynthetic pigments and anti-oxidant activities, the samples at 10 am and 2 pm of day 10 showed a peak in expression. Thus, these two morning hours were selected for isozymes (for further confirmation of scavenging enzymes) and protein analyses. An additional reason behind selecting the morning rhythmic hours was the regulation of PRR genes during the morning (PRR7; PRR9) and at noon (PRR5) [88,89] (during the morning loop) of plant circadian cycles under salinity stress conditions. In a recent study [90], researchers focused on how to explain the connection between the circadian clock and the response of the plant *U. pumila* towards salt stress with the help of physiological and transcriptome variation. The increase in salt concentration in plant leaves also showed an increase in K+ content and decrease in Na+ content.

The frequent changes in environment are perceived by the circadian clock, which transmits temporal information throughout the plant cell in order to synchronize daily and seasonal fluctuations with internal biological processes. Several studies have attempted to study the mechanisms of circadian cellular processes in response to outside environmental conditions such as light, temperature, photoperiodism etc. However, a handful of studies have attempted to observe how the circadian clock can control the cellular processes under abiotic stresses. In this study we briefly discussed recent progress on clock coordination in response to salinity stress in spinach crops. In brief, we found that the circadian clock controls the oxidative damage caused by salinity stress by modulating physiology, antioxidative mechanisms, and the chloroplast proteome, specifically at a circadian time period i.e., 10 am and 2 pm. Although the study provided significant evidence of the circadian clock's ability to control salinity stress, this evidence is only for morning–evening loops; the night loop has still to be studied. Moreover, many aspects of clock control of other important processes such gene-regulatory networks and proteomics as well as protein identifications, and transcription factors are yet to be resolved.

5. Conclusions

Several environmental stresses weaken and damage plants in agricultural production. The breeding of resistant crop resources and improving plant adaptability towards stresses are the key factors for improving crop yield. Circadian core oscillators play a critical role

in plants' perception of and responding to biotic and abiotic stresses, and are, therefore, relevant to future crop production. With the help of current circadian biology in response to salinity stress, it was demonstrated that salt inducibility in the expression of specific salinity-stress related photosynthetic measurements and the plant's proteome is temporally controlled during the day at 10 am and 2 pm in the circadian cycle using spinach genotypes (morning–evening loop). Our investigation of salinity induction in the expression of stress markers, photosynthetic parameters, encoding enzyme activities, and their isozymes was restricted to the morning loop. Our findings not only show the potential importance of further investigating the basis and significance of circadian-controlled salinity stress responses under fluctuating circadian time periods, but also provide the potential to exploit an effective method for improving salinity resistance performance in spinach. In summary, circadian regulation may provide a sophisticated, reliable mechanism for ensuring an optimal balance of plant growth and abiotic stress tolerance. Changes in clock function in response to environmental changes may allow plants to readjust this balance and ensure a sustained increase in abiotic stress tolerance when necessary. The current study can be extended to compare our findings with the night circadian loops to obtain a clear idea about how the dark cycle can overcome the abiotic stress conditions since the present study only focusses on morning–evening loops.

Author Contributions: S.M. conceptualized and supervised the work; A.V. performed the experiments and wrote the draft of the manuscript; D.-W.B. helped in performing protein analysis; S.M. edited and finalized the manuscript. All authors have read and agreed to the published version of the manuscript.

Institutional Review Board Statement: Not applicable.

Data Availability Statement: The data presented in this study are available on request from the author.

Conflicts of Interest: The authors declare no conflict of interest.

References

1. Gupta, B.; Huang, B. Mechanism of salinity tolerance in plants: Physiological, biochemical, and molecular characterization. *Int. J. Genom.* **2014**, *2014*, 701596. [CrossRef] [PubMed]
2. Singh, A. Soil salinity: A global threat to sustainable development. *Soil Use Manag.* **2022**, *38*, 39–67. [CrossRef]
3. Stockle, C.O. Environmental impact of irrigation: A review. In Proceedings of the IV International Congress of Agricultural Engineering. 2002. Available online: https://citeseerx.ist.psu.edu/document?repid=rep1&type=pdf&doi=8321f0dbb29814bd74e6bc858210809ca847a227 (accessed on 15 October 2022).
4. Zhu, Y.x.; Gong, H.J.; Yin, J.L. Role of silicon in mediating salt tolerance in plants: A review. *Plants* **2019**, *8*, 147. [CrossRef]
5. Meng, Y.; Yin, Q.; Yan, Z.; Wang, Y.; Niu, J.; Zhang, J.; Fan, K. Exogenous silicon enhanced salt resistance by maintaining K+/Na+ homeostasis and antioxidant performance in alfalfa leaves. *Front. Plant Sci.* **2020**, *11*, 1183. [CrossRef] [PubMed]
6. Mirza, H.; Nahar, K.; Fujita, M. Plant response to salt stress and role of exogenous protectants to mitigate salt-induced damages. In *Ecophysiology and Responses of Plants under Salt Stress*; Springer: New York, NY, USA, 2013; pp. 25–87.
7. Maduraimuthu, D.; Prasad, P.V. Effects of salinity on ion transport, water relations and oxidative damage. In *Ecophysiology and Responses of Plants under Salt Stress*; Springer: New York, NY, USA, 2013; pp. 89–114.
8. Kumar, S.; Li, G.; Yang, J.; Huang, X.; Ji, Q.; Liu, Z.; Ke, W.; Hou, H. Effect of salt stress on growth, physiological parameters, and ionic concentration of water dropwort (*Oenanthe javanica*) cultivars. *Front. Plant Sci.* **2021**, *12*, 660409. [CrossRef]
9. Evelin, H.; Devi, T.S.; Gupta, S.; Kapoor, R. Mitigation of salinity stress in plants by arbuscular mycorrhizal symbiosis: Current understanding and new challenges. *Front. Plant Sci.* **2019**, *10*, 470. [CrossRef]
10. Klaus, A.; Hirt, H. Reactive oxygen species: Metabolism, oxidative stress, and signaling transduction. *Annu. Rev. Plant Boil.* **2004**, *55*, 373.
11. Triantaphylides, C.; Krischke, M.; Hoeberichts, F.A.; Ksas, B.; Gresser, G.; Havaux, M.; Van Breusegem, F.; Mueller, M.J. Singlet oxygen is the major reactive oxygen species involved in photooxidative damage to plants. *Plant Physiol.* **2008**, *148*, 960–968. [CrossRef]
12. Sharma, P.; Jha, A.B.; Dubey, R.S.; Pessarakli, M. Reactive oxygen species, oxidative damage, and antioxidative defense mechanism in plants under stressful conditions. *J. Bot.* **2012**, *2012*, 1–26. [CrossRef]
13. Nimse, S.B.; Pal, D. Free radicals, natural antioxidants, and their reaction mechanisms. *RSC Adv.* **2015**, *5*, 27986–28006. [CrossRef]

14. Qinghua, S.; Zhu, Z. Effects of exogenous salicylic acid on manganese toxicity, element contents and antioxidative system in cucumber. *Environ. Exp. Bot.* **2008**, *63*, 317–326.

15. Ashraf, M. Biotechnological approach of improving plant salt tolerance using antioxidants as markers. *Biotechnol. Adv.* **2009**, *27*, 84–93. [CrossRef] [PubMed]

16. Sharma, S.S.; Dietz, K.Z. The relationship between metal toxicity and cellular redox imbalance. *Trends Plant Sci.* **2009**, *14*, 43–50. [CrossRef] [PubMed]

17. Ma, L.; Liu, X.; Lv, W.; Yang, Y. Molecular Mechanisms of Plant Responses to Salt Stress. *Front. Plant Sci.* **2022**, *13*, 934877. [CrossRef]

18. Al Murad, M.; Muneer, S. Silicon supplementation modulates physiochemical characteristics to balance and ameliorate salinity stress in mung bean. *Front. Plant Sci.* **2022**, *13*, 1369. [CrossRef]

19. Ayala, A.; Muñoz, M.F.; Argüelles, S. Lipid peroxidation: Production, metabolism, and signaling mechanisms of malondialdehyde and 4-hydroxy-2-nonenal. *Oxidative Med. Cell. Longev.* **2014**, *2014*, 360438. [CrossRef]

20. Young, M.; Kay, S. Time zones: A comparative genetics of circadian clocks. *Nat. Rev. Genet.* **2001**, *2*, 702–715. [CrossRef]

21. Dodd, A.N.; Salathia, N.; Hall, A.; Kevei, E.; Toth, R.; Nagy, F.; Hibberd, J.M.; Millar, A.J.; Webb, A.A.R. Plant circadian clocks increase photosynthesis, growth, survival, and competitive advantage. *Science* **2005**, *309*, 630–633. [CrossRef]

22. Graf, A.; Schlereth, A.; Stitt, M.; Smith, A.M. Circadian control of carbohydrate availability for growth in Arabidopsis plants at night. *Proc. Natl. Acad. Sci. USA* **2010**, *107*, 9458–9463. [CrossRef]

23. Scialdone, A.; Mugford, S.T.; Feike, D.; Skeffington, A.; Borrill, P.; Graf, A.; Smith, A.M.; Howard, M. Arabidopsis plants perform arithmetic division to prevent starvation at night. *Elife* **2017**, *25*, e00669. [CrossRef] [PubMed]

24. Mugford, S.T.; Fernandez, O.; Brinton, J.; Flis, A.; Krohn, N.; Encke, B.; Feil, R.; Sulpice, R.; Lunn, J.E.; Stitt, M.; et al. Regulatory properties of ADP glucose pyrophosphorylase are required for adjustment of leaf starch synthesis in different photoperiods. *Plant Physiol.* **2014**, *166*, 1733–1747. [CrossRef]

25. Webb, A.A.R.; Satake, A. Understanding circadian regulation of carbohydrate metabolism in *Arabidopsis* using mathematical models. *Plant Cell Physiol.* **2015**, *56*, 586–593. [CrossRef] [PubMed]

26. Kumar, K.; Rao, K.P.; Biswas, D.K.; Sinha, A.K. Rice WNK1 is regulated by abiotic stress and involved in internal circadian rhythm. *Plant Signal Behav.* **2011**, *6*, 316–320. [CrossRef]

27. Grundy, J.; Stoker, C.; Carré, I.A. Circadian regulation of abiotic stress tolerance in plants. *Front. Plant Sci.* **2015**, *6*, 648. [CrossRef]

28. Blair, E.J.; Bonnot, T.; Hummel, M.; Hay, E.; Marzolino, J.M.; Quijada, I.A.; Nagel, D.H. Contribution of time of day and the circadian clock to the heat stress responsive transcriptome in Arabidopsis. *Sci. Rep.* **2019**, *9*, 1–12. [CrossRef] [PubMed]

29. Venkat, A.; Muneer, S. Role of Circadian Rhythms in Major Plant Metabolic and Signaling Pathways. *Front. Plant Sci.* **2022**, *13*, 836244. [CrossRef] [PubMed]

30. Xu, Y.; Freund, D.M.; Hegeman, A.D.; Cohen, J.D. Metabolic signatures of *Arabidopsis thaliana* abiotic stress responses elucidate patterns in stress priming, acclimation, and recovery. *Stress Biol.* **2022**, *2*, 11. [CrossRef]

31. Hsu, P.Y.; Harmer, S.L. Wheels within wheels: The plant circadian system. *Trends Plant Sci.* **2014**, *19*, 240–249. [CrossRef]

32. Fan, T.; Aslam, M.M.; Zhou, J.L.; Chen, M.X.; Zhang, J.; Du, S.; Zhang, K.L.; Chen, Y.S. A crosstalk of circadian clock and alternative splicing under abiotic stresses in the plants. *Front. Plant Sci.* **2022**, *13*, 976807. [CrossRef]

33. Morelock, T.E.; Correll, J.C. Spinach. In *Vegetables, I*; Springer: New York, NY, USA, 2008; pp. 189–218.

34. Erfani, F.; Hassandokht, M.R.; Jabbari, A.; Barzegar, M. Effect of cultivar on chemical composition of some Iranian spinach. *Pak. J. Biol. Sci. PJBS* **2007**, *10*, 602–606.

35. Rashid, M.; Yousaf, Z.; Ullah, M.N.; Munawar, M.; Riaz, N.; Younas, A.; Aftab, A.; Shamsheer, B. Genetic variability assessment of worldwide spinach accessions by agro-morphological traits. *J. Taibah Univ. Sci.* **2020**, *14*, 1637–1650. [CrossRef]

36. Correll, J.C.; Morelock, T.E.; Black, M.C.; Koike, S.T.; Brandenberger, L.P.; Dainello, F.J. Economically important diseases of spinach. *Plant Dis.* **1994**, *78*, 653–660. [CrossRef]

37. Delfine, S.; Alvino, A.; Zacchini, M.; Loreto, F. Consequences of salt stress on conductance to CO_2 diffusion, Rubisco characteristics and anatomy of spinach leaves. *Aust. J Plant Physiol.* **1998**, *25*, 395–402.

38. Delfine, S.; Alvino, A.; Villani, M.C.; Loreto, F. Restrictions to carbon dioxide conductance and photosynthesis in spinach leaves recovering from salt stress. *Plant Physiol.* **1999**, *119*, 1101–1106. [CrossRef] [PubMed]

39. Turner, N.C.; Kramer, P.J. *Adaptation of Plant to Water and High Temperature Stress*; Wiley Interscience Pub: New York, NY, USA, 1980; pp. 207–230.

40. Razi, K.; Bae, D.W.; Muneer, S. Target-Based Physiological Modulations and Chloroplast Proteome Reveals a Drought Resilient Rootstock in Okra (*Abelmoschus esculentus*) Genotypes. *Int. J. Mol. Sci.* **2021**, *22*, 12996. [CrossRef] [PubMed]

41. Yang, L.; Tian, D.; Todd, C.D.; Luo, Y.; Hu, X. Comparative proteome analyses reveal that nitric oxide is an important signal molecule in the response of rice to aluminium toxicity. *J. Proteome Res.* **2013**, *12*, 1316–1330. [CrossRef] [PubMed]

42. Hiscox, J.D.; Israelstam, G.F. A method for the extraction of chlorophyll from leaf tissue without maceration. *Candian J Bot.* **1979**, *57*, 1332–1334. [CrossRef]

43. Arnon, J.D.; Israelstam, G.F. Copper enzymes in isolated chloroplast oxidase in *Beta vulgaris*. *Plant Physiol.* **1949**, *42*, 287–292.

44. Bates, L.S.; Waldren, R.P.; Teare, I.D. Rapid determination of free Proline for water-stress studies. *Plant Soil* **1973**, *39*, 205–207. [CrossRef]

45. Heath, R.L.; Packer, L. Photoperoxidation in isolated chloroplast I. Kinetics and stoichiometry of fatty acid peroxidation. *Arch. Biochem. Biophys.* **1968**, *125*, 189–198. [CrossRef]

46. Muneer, S.; Lee, B.R.; Bae, D.W.; Kim, T.H. Changes in expression of proteins involved in alleviation of Fedeficiency by sulfur nutrition in *Brassica napus* L. *Acta Physiol. Plant.* **2013**, *35*, 3037–3045. [CrossRef]

47. Dhindsa, R.S.; Wandekayi, M. Drought tolerance in two mosses: Correlated with enzymatic defence against lipid peroxidation. *J. Exp. Bot.* **1981**, *32*, 79–91. [CrossRef]

48. Nakano, Y.; Asada, K. Hydrogen Peroxide is Scavenged by Ascorbate-specific Peroxidase in Spinach Chloroplasts. *Plant Cell Physiol.* **1981**, *22*, 867–880.

49. Cakmak, I.; Marschner, H. Magnesium deficiency and high light intensity enhance activities of superoxide dismutase, ascorbate peroxidase, and glutathione reductase in bean leaves. *Plant Physiol.* **1992**, *98*, 1222–1227. [CrossRef] [PubMed]

50. Shah, K.; Nahakpam, S. Heat exposure alters the expression of SOD, POD, APX and CAT isozymes and mitigates low cadmium toxicity in seedlings of sensitive and tolerant rice cultivars. *Plant Physiol. Biochem.* **2012**, *57*, 106–113. [CrossRef] [PubMed]

51. Gomes-Junior, R.A.; Moldes, C.A.; Delite, F.S.; Gratão, P.L.; Mazzafera, P.; Lea, P.J.; Azevedo, R.A. Nickel elicits a fast antioxidant response in Coffea arabica cells. *Plant Physiol. Biochem.* **2006**, *44*, 420–429. [CrossRef] [PubMed]

52. Beauchamp, C.; Fridovich, I. Superoxide dismutase: Improved assays and an assay applicable to acrylamide gels. *Anal. Biochem.* **1971**, *44*, 276–287. [CrossRef]

53. Woodbury, W.; Spencer, A.K.; Stahmann, M.A. An improved procedure using ferricyanide for detecting catalase isozymes. *Anal. Biochem.* **1971**, *44*, 301–305. [CrossRef]

54. Clare, D.A.; Duong, M.N.; Darr, D.; Archibald, F.; Fridovich, I. Effects of molecular oxygen on detection of superoxide radical with nitroblue tetrazolium and on activity stains for catalase. *Anal. Biochem.* **1984**, *140*, 532–537. [CrossRef]

55. Anderson, M.D.; Prasad, T.K.; Stewart, C.R. Change in isozyme profiles of catalase, peroxidase, and glutathione reductase during acclimation to chilling in mesocotyls of maize seedlings. *Plant Physiol.* **1995**, *109*, 1247–1257. [CrossRef]

56. Mittler, R.; Zilinskas, B.A. Detection of ascorbate peroxidase activity in native gels by inhibition of the ascorbate-dependent reduction of nitroblue tetrazolium. *Anal. Biochem.* **1993**, *212*, 540–546. [CrossRef] [PubMed]

57. Muneer, S.; Lee, J.H. Hazardous gases (CO, NOx, CH4 and C_3H_8) released from CO_2 fertilizer unit lead to oxidative damage and degrades photosynthesis in strawberry plants. *Sci. Rep.* **2018**, *8*, 12291. [CrossRef] [PubMed]

58. Bradford, M.M. A Rapid and Sensitive Method for The Quantitation of Microgram Quantities of Protein Utilizing the Principal of Protein-Dye Binding. *Ann. Biochem.* **1976**, *72*, 248–254. [CrossRef]

59. Usuda, H. The Activation State of Ribulose 1,5-bisphosphate Carboxylase in Maize Leaves in Dark and Light. *Plant Cell Physiol.* **1985**, *26*, 1455–1463.

60. Muneer, S.; Ko, C.H.; Wei, H.; Chen, Y.; Jeong, B.R. Physiological and proteomic investigations to study the response of tomato graft unions under temperature stress. *PLoS ONE* **2016**, *11*, e0157439. [CrossRef] [PubMed]

61. Muneer, S.; Park, Y.G.; Manivannan, A.; Soundararajan, P.; Jeong, B.R. Physiological and proteomic analysis in chloroplasts of *Solanum lycopersicum L.* under silicon efficiency and salinity stress. *Int. J. Mol. Sci.* **2014**, *15*, 21803–21824. [CrossRef] [PubMed]

62. Ke, M.; Gao, Z.; Chen, J.; Qiu, Y.; Zhang, L.; Chen, X. Auxin controls circadian flower opening and closure in the waterlily. *BMC Plant Biol.* **2018**, *18*, 143. [CrossRef]

63. Sharma, M.; Irfan, M.; Kumar, A.; Kumar, P.; Datta, A. Recent insights into plant circadian clock response against abiotic stress. *J. Plant Growth Regul.* **2021**, *41*, 3530–3543. [CrossRef]

64. Wei, L.-X.; Lv, B.-S.; Li, X.-W.; Wang, M.-M.; Ma, H.-Y.; Yang, H.-Y.; Yang, R.-F.; Piao, Z.-Z.; Wang, Z.-H.; Lou, J.-H.; et al. Priming of rice (*Oryza sativa* L.) seedlings with abscisic acid enhances seedling survival, plant growth, and grain yield in saline-alkaline paddy fields. *Field Crops Res.* **2017**, *203*, 86–93. [CrossRef]

65. Mittler, R.; Vanderauwera, S.; Suzuki, N.; Miller, G.A.D.; Tognetti, V.B.; Vandepoele, K.; Gollery, M.; Shulaev, V.; Van Breusegem, F. ROS signaling: The new wave? *Trends Plant Sci.* **2011**, *16*, 300–309. [CrossRef]

66. Ben Taârit, M.; Msaada, K.; Hosni, K.; Marzouk, B. Fatty acids, phenolic changes and antioxidant activity of clary sage (*Salvia sclarea* L.) rosette leaves grown under saline conditions. *Ind. Crops Prod.* **2012**, *38*, 58–63. [CrossRef]

67. Madany, M.M.Y.; Saleh, A.M. Phytotoxicity of *Euphorbia helioscopia* L. on *Triticum aestivum* L. and *Pisum sativum* L. *Ann. Agr. Sci.* **2015**, *60*, 141–151. [CrossRef]

68. Ashraf, M.; Foolad, M.R. Roles of glycine betaine and proline in improving plant abiotic stress resistance. *Environ. Exp. Bot.* **2007**, *59*, 206–216. [CrossRef]

69. Szabados, L.; Savouré, A. Proline: A multifunctional amino acid. *Trends Plant Sci.* **2010**, *15*, 89–97. [CrossRef]

70. Chookhampaeng, S. The effect of salt stress on growth, chlorophyll content proline content and antioxidative enzymes of pepper (*Capsicum annuum* L.) seedling. *Eur. J Sci. Res.* **2011**, *49*, 103–109.

71. Yasar, F.; Kusvuran, S.; Ellialtıolu, S. Determination of anti-oxidant activities in some melon (*Cucumis melo* L.) varieties and cultivars under salt stress. *J Hort. Sci. Biotechnol.* **2006**, *81*, 627–630. [CrossRef]

72. Ali, S.; Bai, P.; Zeng, F.; Cai, S.; Shamsi, I.H.; Qiu, B.; Wu, F.; Zhang, G. The ecotoxicological and interactive effects of chromium and aluminum on growth, oxidative damage and antioxidant enzymes on two barley genotypes differing in Al tolerance. *Environ. Exp. Bot.* **2011**, *70*, 185–191. [CrossRef]

73. Munns, R. Genes and salt tolerance: Bringing them together. *New Phytol.* **2005**, *167*, 645–663. [CrossRef]

74. Fujita, K.; Ito, J.; Mohapatra, P.K.; Saneoka, H.; Lee, K.; Kurban, H.; Kawai, K.; Ohkura, K. Circadian rhythm of stem and fruit diameter dynamics of Japanese persimmon (Diospyrus kaki Thunb.) is affected by deficiency of water in saline environments. *Funct. Plant Biol.* **2003**, *30*, 747–754. [CrossRef]

75. Rosenqvist, E.; van Kooten, O. Chlorophyll fluorescence: A general description and nomenclature. In *Practical Applications of Chlorophyll Fluorescence in Plant Biology*; DeEll, J.R., Toivonen, P.M.A., Eds.; Kluwer Academic Publishers: Drive Norwell, MA, USA, 2003; pp. 31–37.

76. Withrow, A.P.; Withrow, R.B. Photoperiodic chlorosis in tomato. *Plant Physiol.* **1949**, *24*, 657–663. [CrossRef] [PubMed]

77. Hennessey, T.L.; Arthur, L.F.; Christopher, B.F. Environmental effects on circadian rhythms in photosynthesis and stomatal opening. *Planta* **1993**, *189*, 369–376. [CrossRef]

78. Rao, G.G.; Rao, G.R. Pigment composition and chlorophyllase activity in pigeon pea (Cajanus indicus Spreng) and Gingelley (*Sesamum indicum* L.) under NaCl salinity. *Indian J. Exp. Biol.* **1981**, *19*, 768–770.

79. Noreen, Z.; Ashraf, M. Changes in antioxidant enzymes and some key metabolites in some genetically diverse cultivars of radish (*Raphanus sativus* L.). *Environ. Exp. Bot.* **2009**, *67*, 395–402. [CrossRef]

80. Smirnoff, N. Botanical briefing: The function and metabolism of ascorbic acid in plants. *Ann. Bot.* **1996**, *78*, 661–669. [CrossRef]

81. Sevengor, S.; Yasar, F.; Kusvuran, S.; Ellialtioglu, S. The effect of salt stress on growth, chlorophyll content, lipid peroxidation and antioxidative enzymes of pumpkin seedling. *Afr. J. Agric. Res.* **2011**, *6*, 4920–4924.

82. Turan, M.A.; Turkmer, N.; Taban, N. Effect of NaCl on stomatal resistance and proline chlorophyll, NaCl and K concentrations of lentil plants. *J Agron.* **2007**, *6*, 378–381. [CrossRef]

83. Taffouo, V.D.; Wamba, O.F.; Yombi, E.; Nono, G.V.; Akoa, A. Growth, yield, water status and ionic distribution response of three bambara groundnut (*Vigna subterranean* (L.) verdc.) landraces grown under saline conditions. *Int. J of Bot.* **2010**, *6*, 53–58. [CrossRef]

84. Verma, S.; Mishra, S.N. Putrescine alleviation of growth in salt stressed Brassica juncea by inducing antioxidative defense system. *J. Plant Physiol.* **2005**, *162*, 669–677. [CrossRef]

85. Taïbi, K.; Taïbi, F.; Abderrahim, L.A.; Ennajah, A.; Belkhodja, M.; Mulet, J.M. Effect of salt stress on growth, chlorophyll content, lipid peroxidation and antioxidant defence systems in *Phaseolus vulgaris* L. *South Afr. J. Bot.* **2016**, *105*, 306–312. [CrossRef]

86. Wahid, A.; Gelani, S.; Ashraf, M.; Foolad, M. Heat tolerance in plants: An overview. *Environ. Exp. Bot.* **2007**, *61*, 199–223. [CrossRef]

87. Muneer, S.; Ko, C.H.; Soundararajan, P.; Manivnnan, A.; Park, Y.G.; Jeong, B.R. Proteomic Study Related to Vascular Connections in Watermelon Scions Grafted onto Bottle-Gourd Rootstock under Different Light Intensities. *PLoS ONE* **2015**, *10*, e0120899. [CrossRef] [PubMed]

88. Matsushika, A.; Makino, S.; Kojima, M.; Mizuno, T. Circadian waves of expression of the APRR1/TOC1 family of pseudo-response regulators in Arabidopsis thaliana: Insight into the plant circadian clock. *Plant Cell Physiol.* **2000**, *41*, 1002–1012. [CrossRef] [PubMed]

89. Nakamichi, N.; Kiba, T.; Henriques, R.; Mizuno, T.; Chua, N.H.; Sakakibara, H. Pseudo-response regulators 9, 7, and 5 are transcriptional repressors in the Arabidopsis circadian clock. *Plant Cell.* **2010**, *22*, 594–605. [CrossRef] [PubMed]

90. Chen, P.; Liu, P.; Zhang, Q.; Zhao, L.; Hao, X.; Liu, L.; Bu, C.; Pan, Y.; Zhang, D.; Song, Y. Dynamic physiological and transcriptome changes reveal a potential relationship between the circadian clock and salt stress response in *Ulmus pumila*. *Mol. Genet. Genom.* **2022**, *297*, 303–317. [CrossRef] [PubMed]